1 **Body size trends and recovery amongst bivalves following the end-Triassic**

2 **mass extinction**

3 **Jed W. Atkinson* and Paul B. Wignall**

4 **School of Earth and Environment, University of Leeds, Leeds, UK, LS2 9JT.**

5 ***gy12jwa@leeds.ac.uk**

6 **Abstract**

7 **Fossils in the immediate aftermath of mass extinctions are often of**

8 **small size, a phenomenon attributed to the Lilliput Effect (temporary, size**

9 **reduction of surviving species). There has been little attempt to study size**

10 **trends during subsequent recovery intervals nor has the relationship between**

11 **size, diversity and environmental controls been evaluated. Here we examine**

12 **the recovery following the end-Triassic mass extinction amongst bivalves of**

13 **the British Lower and Middle Lias. Three distinct phases of size change are**

14 **seen that are independent of other recovery metrics: initially bivalves are small**

15 **but the Lilliput Effect is a minor factor, the majority of small taxa belong to new**

16 **species that undergo a later within-species size increase (the Brobdingnag**

17 **Effect) throughout the subsequent Hettangian Stage. New species that**

18 **appeared during the Hettangian were also progressively larger and Cope's**

19 **Rule (size increase between successive species) is seen – notably amongst**

20 **ammonites. The size increase was reversed during the Sinemurian Stage,**

21 **when bivalves once again exhibited small body sizes. During the**

22 **Pliensbachian Stage another phase of size increase occurred with further**

23 **evidence of the Brobdingnag Effect. These three phases of size change are**

24 **seen across all suspension feeding ecological guilds of bivalve but are not**

25 **expressed among deposit feeders. Local environmental conditions explain**

26 **some aspects of size patterns, but factors such as temperature, marine**

27 **oxygenation and sea level, do not correlate with the long-term size trends. The**

28 **Brobdingnag Effect may reflect increased availability/quality of food during the**

29 **recovery interval: a factor that controlled bivalve size but not evolution.**

30

31 **Keywords: Brobdingnag Effect; Lilliput Effect; Cope's Rule; Lower Jurassic**

32 **palaeoenvironments**

33

34 1. Introduction

35   The causes and nature of size changes during mass extinction events have

36 been much debated (Atkinson et al., 2019; Brayard et al., 2010; Brom et al., 2015;

37 Chen et al., 2019; Harries and Knorr, 2009; Metcalfe et al., 2011; Sogot et al., 2014;

38 Song et al., 2011; Twitchett, 2007; Wiest et al., 2018). Species that survive mass

39 extinctions are often unusually small and are termed "Lilliput taxa" (Urbanek, 1993),

40 although the more general term "Lilliput Effect" is used to describe the prevalence of

41 smaller species at this time. The cause of the size reduction is often unclear and

42 there are several possible mechanisms including preferential extinction of large taxa,

43 dwarfing of species that cross the extinction boundary and proliferation of small,

44 fecund species (opportunists) in the high stress conditions of the extinction interval

45 (Batten and Stokes, 1986; Harries and Knorr, 2009; Payne, 2005; Twitchett, 2007).

46 Implicit in the Lilliput concept is that species return to larger sizes in the subsequent

47 post-extinction interval as the stressful conditions ameliorate. However, a recent

48 study of sizes changes in limid bivalves in the aftermath of the end-Triassic mass

49 extinction revealed a prolonged size increase of species that first appeared after the

50 extinction but with no precursory size reduction (Atkinson et al., 2019). This has

51 been termed the Brobdingnag Effect, after the race of giants in *Gulliver's Travels*,

52 and its importance during post-extinction recovery remains unexplored. The

53 Brobdingnag Effect is an intraspecific size increase and is thus distinct from Cope's

54 Rule which is an increase in size between successive species in a lineage (Alroy,

55 1998; Cope, 1887; Jablonski, 1997; Rensch, 1948).

56   Here we examine the size-recovery relationships of the bivalve fauna from the

57 British Rhaetian (Upper Triassic) to Pliensbachian (Lower Jurassic) to determine the

58 extent of the Brobdingnag Effect and its possible causes following the end-Triassic

59 mass extinction event. Body size of marine invertebrates is influenced by factors like

60 water temperature, dissolved oxygen content, salinity and nutrient availability (e.g.

61 Atkinson, 1994; His et al., 1989; Rhoads and Morse, 1971; Wacker and von Elert,

62 2008). It is likely that each species responds to environmental changes in their own

63 unique manner with each species having a different optimal body size for a certain

64 environment (Carey and Sigwart, 2014; Hallam, 1965).

65   Oxygen restriction has been demonstrated as a cause of reduced body sizes

66 (Rhoads and Morse, 1971; Richmond et al., 2006) due to reduced metabolic and

67 growth rates (Richmond et al., 2006), although some low-oxygen tolerant species

68 can increase in size as oxygen levels decline (Wignall, 1990). Temperature exerts a

69 control on the concentration of dissolved gasses within the waters, but it can also

70 affect body size directly. Perhaps the most renowned temperature-size trend is

71 Bergmann's Rule, although this is strictly a positive correlation with body size and

72 latitude – taken as an approximation of temperature (Bergmann, 1847; Blackburn et

73 al., 1999; James, 1970). As the current study has little in the way of a latitudinal

74 gradient it is perhaps better, in order to avoid confusion, to refer to the rather

75 unambiguously named Temperature-Size Rule (Atkinson, 1994; Atkinson and Sibly,

76 1997). This rule explains how growth rates and development rates are affected

77 unequally by temperature with the latter being more sensitive. For example, under

78 low temperatures both growth and development rates are slowed, the latter more so

79 thereby delaying sexual maturity allowing an increased duration of growth which can

80 result in larger animals.

81   Food availability and quality are known controls on body size (von Elert et al.,

82 2003; Wacker and von Elert, 2003). Amongst bivalves, red algae (dinoflagellates)

83 are preferable for good growth over green algae (prasinophytes and acritarchs)

84 because the latter are smaller which reduces the capture rate by the gills of bivalves,

85 and also green algae lack key long-chained polyunsaturated fatty acids essential for

86 growth (Brown et al., 1997; von Elert et al., 2003; Weiss et al., 2007). Turbidity of the

87 water has also been suggested as a factor affecting body size because it lowers

88 filtration rate in the bivalves, and causes them to spend more time with valves closed

89 (Loosanoff and Tommers, 1948).

90   Single species distributed over a broad range of water depths are often

91 (although not exclusively) smaller at greater bathymetries (Attrill et al., 1990;

92 Kaariainen and Bett, 2006; Olabarria and Thurston, 2003). This is likely a

93 manifestation of numerous depth-linked factors such as food and dissolved oxygen

94 concentrations (Peck and Harper, 2010; Shi et al., 2016; Shirayama, 1983).

95   Most of the size-control factors that are outlined above can be evaluated in

96 the geological record and are considered here in order to distinguish environmental

97 controls from temporal trends in bivalve body size in the Lower Jurassic following the

98 end-Triassic mass extinction.

99

2. Geological setting

During the Rhaetian and Lower Jurassic the British Isles formed part of an epicontinental sea that extended across much of northwest Europe (Hallam, 1960). The Rhaetic sea was likely of variable salinity, as it lacked stenohaline taxa (Hallam and El Shaarawy, 1982; Swift, 1999). Fully marine conditions developed around the Triassic-Jurassic boundary and persisted into the Lower Jurassic. Many islands dotted this Jurassic sea, and consequently a range of depositional environments are recorded across different basins in relation to proximity to these landmasses (Fig. 1). For example the Bristol Channel Basin passes onto the Welsh Massif, where Carboniferous limestones are onlapped by marginal facies (Sheppard, 2006). Likewise, there are similar facies around the Shepton Mallet area of Somerset (Simms, 2004).

112
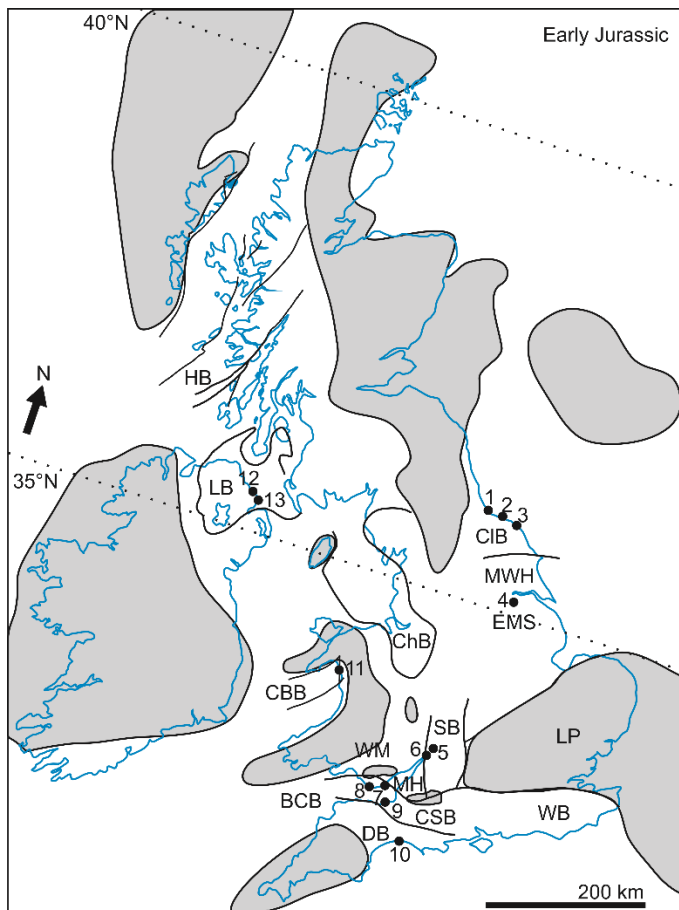
Fig. 1 Palaeogeography of the British Isles with Hettangian landmasses (indicated by shaded regions) and sedimentary basins. Based on Copestake and Johnson (2014); Deconinck et al. (2003); Lindström et al. (2017); Martill et al. (2016); Simms et al. (2004). Codes as follows: HB – Hebrides Basin; LB – Larne Basin; ClB – Cleveland Basin; MWH – Market Weighton High; EMS – East Midlands Shelf; ChB – Cheshire Basin; CBB – Cardigan Bay Basin; BCB – Bristol Channel Basin; CSB – Central Somerset Basin; SB – Severn Basin; WM – Welsh Massif; WB – Wessex Basin; MH – Mendips High; DB – Dorset Basin; LP – London Platform. Location numbers (numbers in parenthesis after locality names use British National Grid reference systems): 1 – Redcar, North Yorkshire (NZ 613 253); 2 – Staithes, North Yorkshire (NZ 781 190); 3 – Hawsker Bottoms (NZ 952 076) and Robin Hood's Bay, North Yorkshire (NZ 971

028); 4 – Conesby Quarry, Scunthorpe (SE 889 145); 5 – Robin's Wood Hill Quarry, Gloucestershire (SO 835 148); 6 – Hock Cliff, Gloucestershire (SO 725 093); 7 – Lavernock Point, Glamorgan (ST 188 682 – ST183.679); 8 – Nash Point, Glamorgan (SS 911 692 – SS 921 679); 9 – Doniford (ST 083 431), St Audire's Bay (ST 103 434 – ST 099 433), East Quantoxhead to Kilve (ST 134 442 – 142 444), and Lilstock (ST 178 453), Somerset; 10 – Pinhay Bay to Charmouth (SY 317 907 – SY 970 929), Devon/Dorset; 11 – Llanbedr (Mochras Farm) borehole, north Wales (SH 553 259); 12 – Larne (NW 558 582) and Portmuck Harbour (NW 558 582) County Antrim; 13 – Cloghfin Port (NW 624 490) and Cloghfin Point (NW 608 454), County Antrim.

There were, broadly speaking, four phases of sedimentation in the British Rhaetian to Middle Lias (outlined below). Between the basins and shelves these intervals are correlated using a well-defined ammonite biostratigraphy (Fig. 2).
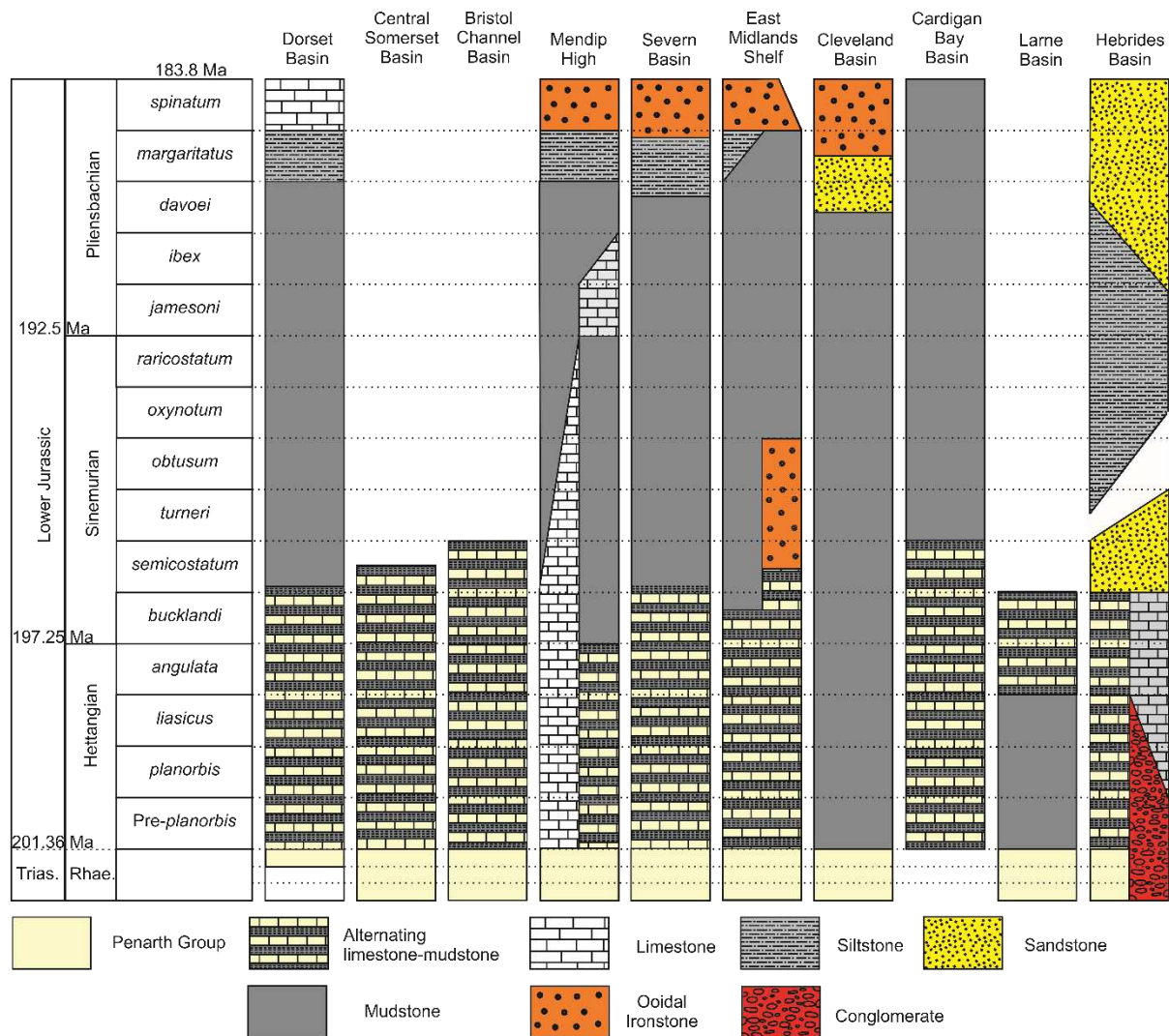
Fig.2 Schematic lithostratigraphy of studied sedimentary basins with ammonite chronozone scheme and geological stages. Modified from Ivimey-Cook (1971); Simms et al. (2004); Simms and Jeram (2007). Stage boundary ages from Ruhl et al. (2016); Weedon et al. (2019); Wotzlaw et al. (2014).

Rhaetic sedimentation in the British Isles is recorded in the Penarth Group, consisting of the shallow-water, quasimarine Westbury and Lilstock formations. The Lilstock Formation comprises the Cotham and Langport members with the end-Triassic mass extinction occurring in the Cotham Member during a regressive interval (Wignall and Bond, 2008). Subsequent deposition saw progressive

150 deepening, although a minor sea-level fall occurred at the top of the Group (Wignall,

151 2001). An alternative lithostratigraphical scheme has been proposed for the Rhaetian

152 stratigraphy by Gallois (2009) whereby the Cotham Member has been elevated to

153 rank of formation and the Langport Member is disbanded into two formations: the

154 White Lias and Watchet Mudstone.

155   Pre-planorbis to bucklandi chonozones sees the onset of the Blue Lias

156 Formation, a cyclic limestone-marl-shale unit that represents offshore deposition

157 (Hallam, 1960; Moghadam and Paul, 2000; Weedon, 1986). In the liasicus

158 Chronozone limestone beds are rarer – likely due to deepening (Ivimey-Cook, 1975;

159 Weedon et al., 2018). The cycles reflect orbitally-paced climate oscillations and

160 approximately correspond to fluctuations in marine redox (Atkinson and Wignall,

161 2019; Moghadam and Paul, 2000; Ruhl et al., 2010; Weedon et al., 2019, 2018). The

162 Blue Lias Formation is found chiefly in southern regions of Britain, and passes

163 northwards into mudstone-dominated successions (Fig. 2; Simms and Page 2004).

164 However, the Blue Lias is also developed in the Hebrides Basin of north-west

165 Scotland where it passes laterally into the shallower-water bioclastic limestones of

166 the Breakish or Broadford Formation (Oates, 1978).

167   Mudstone dominates sedimentation from the semicostatum to davoei

168 chronozones (e.g. the Charmouth Mudstone, Redcar Mudstone and Pabay Shale

169 formations; Fig. 2). Within the semicostatum to obtusum interval deposition within the

170 Dorset Basin is characterised by sediments of high organic carbon content and

171 evidence for sea-floor anoxia, these being the Shales-with-Beef and Black Ven Marls

172 of the Charmouth Mudstone Formation (Gallois, 2008; Wignall and Hallam, 1991).

173 Similarly the obtusum Chronozone of the Mendips is represented by dark laminated

174 limestones (Simms, 2004). To the north of this region lithologies are more variable.

175　The northern part of the East Midlands Shelf (EMS) is especially distinct during the

176　semicostatum to obtusum chronozones with the deposition of the Frodingham

177　Ironstone Member of the Scunthorpe Mudstone Formation (Hallam, 1963).

178　Deposition in the Hebrides Basin during this interval was dominated by siltstones of

179　the misleadingly named Pabay Shale Formation (Morton, 1989; Oates, 1978).

180　Deposition here occurred under shallower water depths than seen in several basins

181　at this time and was above the storm wave-base (Morton and Oates, 2004).

182

183　　　Siltstone deposition dominated the davoei to margaritatus interval across

184　much of the British Isles (Fig. 2). Once again in the Hebrides Basin conditions were

185　shallower than elsewhere indicated by the Scalpay Sandstone Formation (Donovan

186　et al., 2005; Hesselbo et al., 1998; Radley, 2003). Within the Cleveland Basin the

187　later part of this interval saw the Staithes Sandstone Formation replaced by the

188　Cleveland Ironstone Formation, that shows coarsening-up cycles capped by oolitic

189　ironstone beds (Howard, 1985; Howarth, 1955). Indeed, many basins show an

190　overall coarsening upwards during this interval that culminates in the spinatum

191　Chronozone (Fig. 2). This is not expressed in the Cardigan Bay Basin however,

192　where siltstone dominates the succession from the jamesoni Chronozone upwards

193　(Ivimey-Cook, 1971).

194

195　**3. Materials and methods**

196　　　Bivalve size data were collected from the Westbury Formation to the topmost

197　spinatum Chronozone, encompassing the Rhaetian, Hettangian, Sinemurian and

198　Pliensbachian stages. The bivalves Plagiostoma giganteum J. Sowerby and all

199　species of Gryphaea were excluded from our analysis because their size trends are

200   already well-documented (Atkinson et al., 2019; Hallam, 1978; Johnson, 1994).

201   Latest Rhaetian and Liassic (Lower to Middle) bivalve data were collected via two

202   methods: direct field observations and museum collections. Field collections were

203   made from coastal locations in Devon, Dorset, Somerset, Glamorgan, North

204   Yorkshire, and County Antrim, a river cliff section and quarry in Gloucestershire, a

205   quarry in north Lincolnshire and material retrieved from the Llanbedr (Mochras Farm)

206   borehole, Wales housed in the British Geological Survey, Keyworth, Nottingham

207   (Fig. 1). These sections represent the full spectrum of sedimentary basins and

208   depositional settings of the epicontinental sea that covered much of the British Isles

209   in the Early Jurassic. For softer lithologies (mudstones, siltstones, shales and marls),

210   fossils were measured and collected from freshly split surfaces from approximately

211   equal volumes of rock (50 x 50 cm area and 20-30 cm depth). For the harder

212   limestone and ironstone beds, which could not easily be split, fossils were measured

213   in situ from upper bedding surfaces or from scree if zonal affinity could be confirmed.

214   Museum collections include specimens with sufficient biostratigraphic context

215   from the following institutes: National Museum of Wales, Cardiff (NMW);

216   Warwickshire Museum, Warwick (WARMS); Bristol City Museum and Art Gallery,

217   Bristol (BRSMG); Yorkshire Museum, York (YORYM); Whitby Museum, Whitby

218   (WHITM); Bath Royal Literary and Scientific Institute, Bath (BRLSI). In addition,

219   personal collections made by Michael Oates and JWA from the Hebrides Basin,

220   material from Blockley Station Quarry, Long Itchington Quarry and Somerset

221   collected previously by PBW housed in the School of Earth and Environment,

222   University of Leeds and specimens from Northern Ireland donated by Michael

223   Simms, are included. These are amalgamated under 'museum collections' as no

224   conscious effort to avoid size biased sampling could be guaranteed.

225   For each specimen a series of measurements were recorded (Fig. 3) using a

226   pair of digital callipers with a measurement error of +/-0.02 mm. For inequivalved

227   species the larger valve was measured. Growth line spacing was measured from

228   high resolution photographs in order to assess changes in growth rates. Height and

229   length measurements were used to calculate geometric mean body size (GMBS).

230   This being the square root of the product of height and length. For incomplete

231   specimens the missing values are calculated based on height to length ratios of

232   coeval, complete specimens.
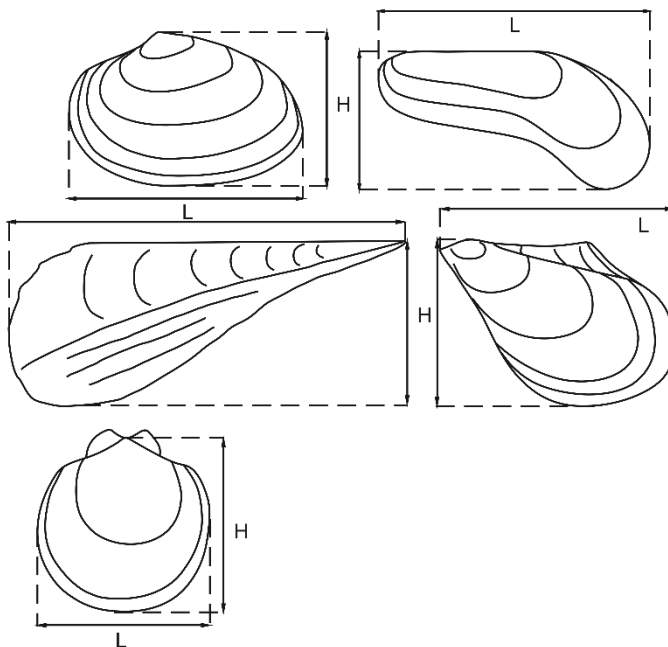
233

234   **Fig. 3 Measurement schematic for a variety of bivalve morphologies.**

235

236   GMBS is used for size analysis as it provides a better representation of a

237   specimen's overall size than a single linear measurement, and correlates well with

238   other, more complex, body size measurements, whilst being easy to obtain (cf.

239   Kosnik et al., 2006).

240   Ammonite chronozones are selected for time bins providing a high-resolution

241   age model suitable for both museum specimens (with sufficient context), and field

242   observations. In some instances, data from the semicostatum and turneri

243   chronozones were pooled, owing to low sample sizes. Durations of ammonite

244   chronozones (including Pre-planorbis Beds) are primarily from astrochronological

245   timescales of Ruhl et al. (2016) and Weedon et al. (2019) with the exception of the

246   interval spanning the semicostatum to oxytonum chronozones, duration for these

247   chronozones are based on the assumption of equal duration of subchronozones. For

248   the Rhaetian, which lacks ammonites, the Westbury Formation, Cotham Member

249   (equivalent to Cotham Formation) and Langport Member (equivalent to White Lias

250   and Watchet Mudstone formations) are used as time bins, although these are of

251   uncertain durations. The resultant floating chronology is tied using the U-Pb

252   radiometric dates for the end-Triassic mass extinction and Triassic-Jurassic

253   boundary of Wotzlaw et al. (2014).

254   Size plots feature mean GMBS and maximum GMBS per time bin. Error bars

255   on mean body size depict 95% confidence interval, representing the range of

256   population body sizes. Maximum body size is herein referring to mean of the largest

257   10% of the population, rather than the single largest specimen and is only calculated

258   when n ≥ 10. This approach was used in order to reduce the effects of abnormally

259   large outliers (Johnson, 1994). Percentage size changes are quoted relative to the

260   size in the previous time bin, unless otherwise stated. The autecology of each

261   species is assigned using a modified version of the scheme presented in Ros-Franch

262   et al. (2014) (See supplementary appendix 1).

263   Where sufficient sample sizes are available from an ammonite chronozone,

264   size differences between locations (and thereby environment) are considered. For

265   species present within the Blue Lias Formation there is a further test as a single

266   ammonite chronozone at a single location may encompass a variety of lithologies

267   (Atkinson and Wignall, 2019). In order to test for the effects of lithology related

268   variation on body size, specimens were divided into samples from limestones, pale

269   marls, dark marls and shales:- the succession of lithologies seen in the Blue Lias

270   Formation that broadly correspond to progressively decreasing oxygenation

271   (Atkinson and Wignall, 2019; Moghadam and Paul, 2000).

272   Additionally, body size of specimens housed in museum collections are

273   compared to field observations in order to test for size bias and assess the usability

274   of the wealth of material housed in museums for these such studies. Statistical

275   significance of size changes between time bins is shown using a Kolmogorov-

276   Smirnov test (K-S test) and for correlations a Spearman's Rank test, p-values are

277   quoted with a 95% significance threshold ($p < 0.05$). These analyses were carried

278   out using PAST 3.12 statistical software (Hammer et al., 2001). All other analyses

279   were carried out using Microsoft Office Excel 2013.

280

281   **4. Results**

282   4.1 All bivalves

283   A total of 6564 bivalve specimens, belonging to 147 species, were measured

284   (Supplementary appendix 2). When the entire dataset is plotted three distinct phases

285   of size change can be seen: the Westbury Formation to the angulata Chronozone;

286   bucklandi to oxynotum chronozones and raricostatum to spinatum chronozones. The

287   first phase is one of increasing body size (Fig. 4A). Over this interval maximum size

288   increases by 195%. Mean size increases also, this reaches a plateau of 23-25 mm

289   from the liasicus to bucklandi Chronozone. Between the Westbury Formation and the

290   liasicus Chronozone mean body size increases by 182%. During this phase newly

291   appearing taxa are typically larger within successive time bins (Fig. 4B).

292   The second phase spans much of the Sinemurian Stage. This period saw a

293   decline in maximum body size that began in the bucklandi Chronozone and

294   continued into the semicostatum Chronozone (Fig. 4A). From the body size peak in

295   the angulata Chronozone to the semicostatum Chronozone the maximum size of

296   bivalves fell by 47% resulting in a return to body sizes seen in the Pre-planorbis

297   Beds. Mean body size only decreases after the bucklandi Chronozone but still shows

298   a Sinemurian trough. The few newly originating species in this interval are typically

299   smaller than those that originated during the Hettangian (Fig. 4B). The prolonged

300   period of low body sizes is punctuated by a positive spike in both maximum and

301   mean size centred on the obtusum Chronozone (Fig. 4A). This produces a mean

302   body size 32% larger than the liasicus Chronozone and returns maximum body size

303   to a par with those seen during the angulata Chronozone.

304   The third phase corresponds broadly to the Pliensbachian Stage (but also

305   includes the last ammonite chronozone of the Sinemurian) and saw body size

306   increase again (Fig. 4A). Mean body size rises progressively from the oxynotum

307   Chronozone to the ibex Chronozone, increasing by 234%. Maximum size also shows

308   this increase into the ibex Chronozone increasing by 155%, however this is less

309   gradual with a near doubling of size occurring between the oxynotum and

310   raricostatum chronozones. There then follows a shallow depression of both mean

311   and maximum size (however these remain higher than much of the Hettangian and

312   Sinemurian) until the culmination of the Pliensbachian Stage size increase in the

313   spinatum Chronozone, when maximum size attained 115.2 mm.

314   During the entire study interval (Westbury Formation to spinatum

315   Chronozone) maximum size of bivalves increases by 347% and mean size by 328%,

316   with an overall average bivalve body size of 19.1 mm. The typical maximum size of

317   the same interval is 57.6 mm. The angulata, obtusum and raricostatum-spinatum

318   chronozones have a maximum size that is larger than the average for the Lower-

319   Middle Lias.

320   Body size and bivalve diversity exhibit no significant correlation (mean size

321   and diversity $r = +0.23$, $p = 0.35$; maximum size and diversity $r = +0.29$, $p = 0.25$;

322   Fig. 4A). Diversity drops in the Cotham Member due to the end-Triassic mass

323   extinction event and is followed by a diversity increase (albeit with a slight decline in

324   the Pre-planorbis Beds), that continues to the semicostatum Chronozone, after

325   which it declines to between 40-45 species. This stability continues to the davoei

326   Chronozone and then begins to decline.
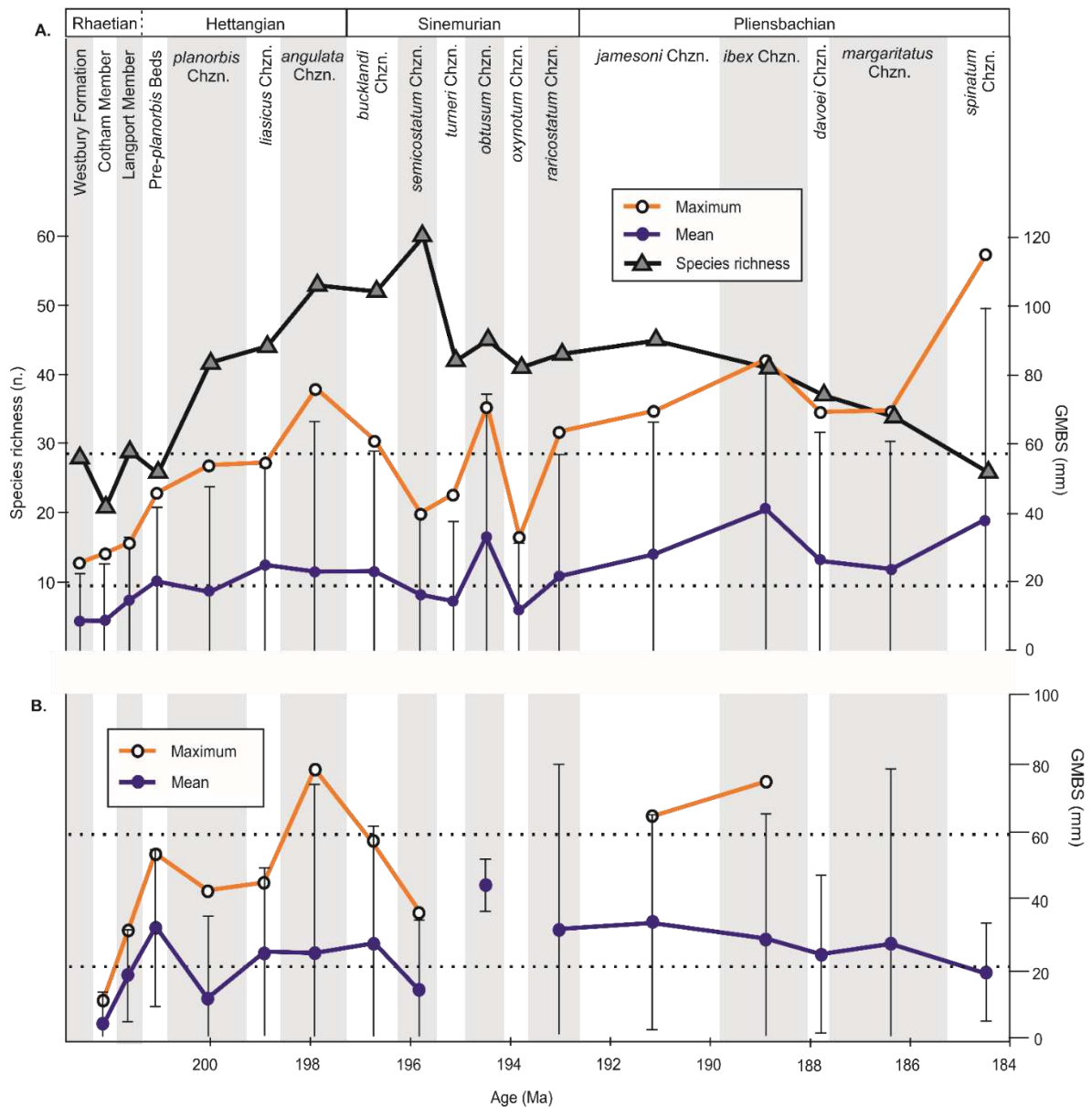
Fig. 4 Time-binned geometric mean size plots for all Rhaetian and Lower Jurassic bivalves, hollow circles depict maximum size (see methods), filled circles show mean bivalve size, error bars show 95% confidence interval representing range of sizes within a time bin. Dashed horizontal lines show Lower-Middle Lias average for maximum and mean size. A, All bivalves measured per time bin, additionally bivalve species richness per time bin (grey triangles). B, size of newly arriving bivalve species per chronozone.

336   4.2 Basin trends

337   A Rhaetian to latest Hettangian size increase is seen within most of the
338   basins studied, although the magnitude of the increase and precise timing of the
339   peak varies slightly (Fig. 5A-D). The Dorset Basin and Mendip High (and surrounding
340   areas) exhibit a peak size in the liasicus Chronozone, indeed bivalves from this latter
341   region are the largest of the entire study. For the Bristol Channel Basin – Welsh
342   Massif and Larne Basin the largest bivalves were encountered in the angulata
343   Chronozone, whilst in the Hebrides Basin and EMS these occur in the bucklandi
344   Chronozone. Large bivalves were not encountered in every basin, bivalves are
345   consistently small in the Central Somerset and Cardigan Bay basins and do not
346   show the Hettangian phase of size increase (Fig. 5D).

347   Size troughs are seen in many of the basins following the Hettangian (or
348   earliest Sinemurian) size maxima (Fig. 5A-D). There is a well-developed depression
349   in the mean body size of bivalves from the Cleveland Basin from the semicostatum
350   Chronozone to the raricostatum Chronozone although, in most basins, this decrease
351   is poorly constrained because the sample size diminishes after the semicostatum
352   Chronozone. Nonetheless the decline is seen in the Mendips, Bristol Channel Basin-
353   Welsh Massif and the Dorset Basin when bivalve size returns to values similar to
354   those of the Penarth Group. The size decrease is even noted on the EMS, following
355   a high in the bucklandi Chronozone (when bivalves are the largest of any of the
356   British basins). It should also be noted that even with a size reduction the bivalves of
357   the EMS from the semicostatum and obtusum chronozones remain the largest of any
358   of the basins and were collected from the Frodingham Ironstone Member of the
359   Scunthorpe Mudstone Formation.

360   A phase of size increase during the Pliensbachian is clearly seen in the

361   Cleveland Basin, starting from the jamesoni Chronozone and culminating with

362   bivalves over 100 mm from the spinatum Chronozone (similar spinatum Chronozone

363   sizes are recorded from the Hebrides Basin). Although sampling is sporadic during

364   the Pliensbachian from many of the basins, when sampled, there is a fairly

365   consistent occurrence of large bivalves from the ibex Chronozone (Dorset, Severn,

366   and Cardigan Bay basins).
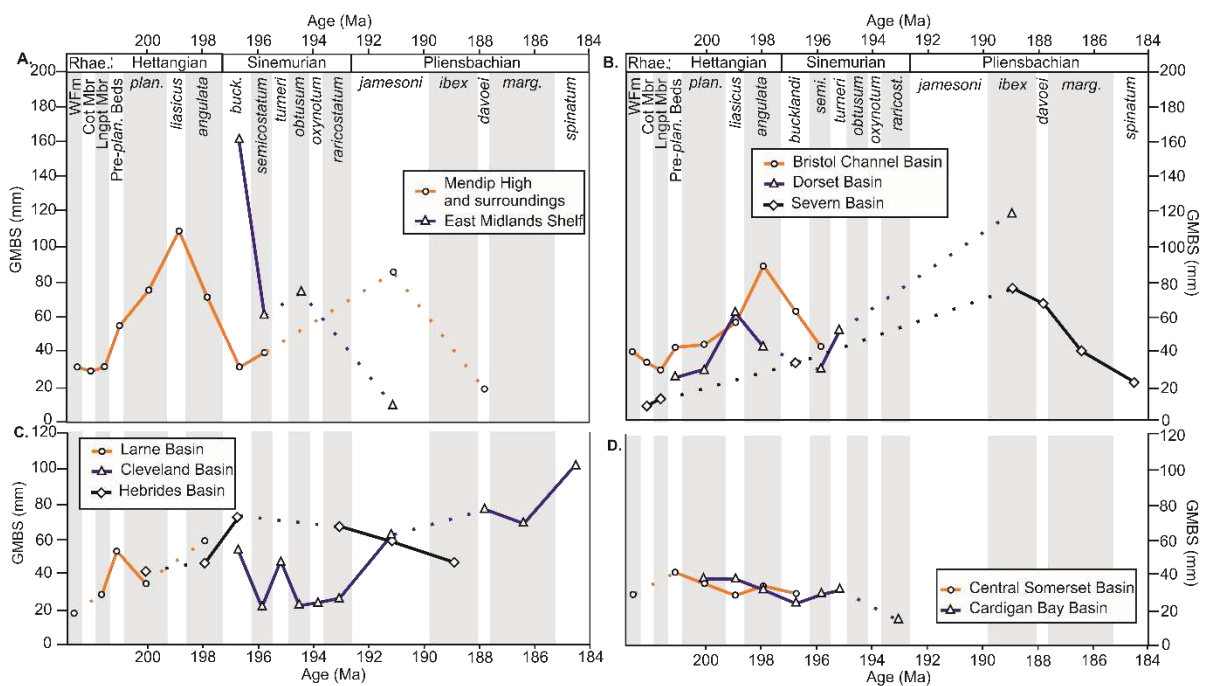
367

368   **Fig. 5A-D Maximum GMBS of bivalves per time bin per basin/shelf. Time bin**

369   **abbreviations: WFm – Westbury Formation; Cot Mbr – Cotham Member; Lngpt**

370   **Mbr – Langport Member; Pre-plan. Beds – Pre-planorbis Beds; plan. –**

371   **planorbis Chronozone; buck. – bucklandi Chronozone; marg. – margaritatus**

372   **Chronozone. See individual legends for basin information.**

373

374   4.3 Trends within ecological groups

375   Within the majority of the ecological guilds employed by bivalves, the three

376   main size phases can be readily noted. All recorded suspension feeding guilds,

377   irrespective of attachment style or burrow depth show a size increase in both mean

378   and maximum body size from the Rhaetian and across the Hettangian (Fig. 6A). A

379   suppressed body size during the Sinemurian is best expressed in endo- and

380   epibyssate suspension feeding bivalves (Fig. 6A). This trend is weaker in shallow

381   infaunal suspension feeders and cementing bivalves, and is however first expressed

382   earlier during the angulata Chronozone. The brief obtusum Chronozone reversal of

383   the size decline is exhibited only in shallow infaunal and epibyssate suspension

384   feeders. The third phase, a Pliensbachian size increase is again seen in all

385   suspension feeding guilds of bivalve (except cementing bivalves), however

386   epibyssate bivalves show a maximum and mean peak size centred on the ibex

387   Chronozone, with later Pliensbachian members of this ecology being progressively

388   smaller.

389   Shallow infaunal, deposit feeding bivalves show fundamentally different size

390   trends to the suspension feeders (Fig. 6B). Thus, there is no Hettangian size

391   increase, instead mean size is similar between the planorbis and angulata

392   chronozones (~10 mm) whilst maximum size decreases slightly (18%). Mean body

393   size decreases from the angulata to the bucklandi Chronozone, while the maximum

394   size remains the same. During the obtusum Chronozone mean and maximum sizes

395   are comparable to the planorbis Chronozone and for the Pliensbachian mean body

396   size remains around 10 mm and maximum, as seen within the planorbis and

397   obtusum chronozones, remains around 20 mm, only seeming large due to a decline

398   in both mean and maximum size in the jamesoni Chronozone.

399
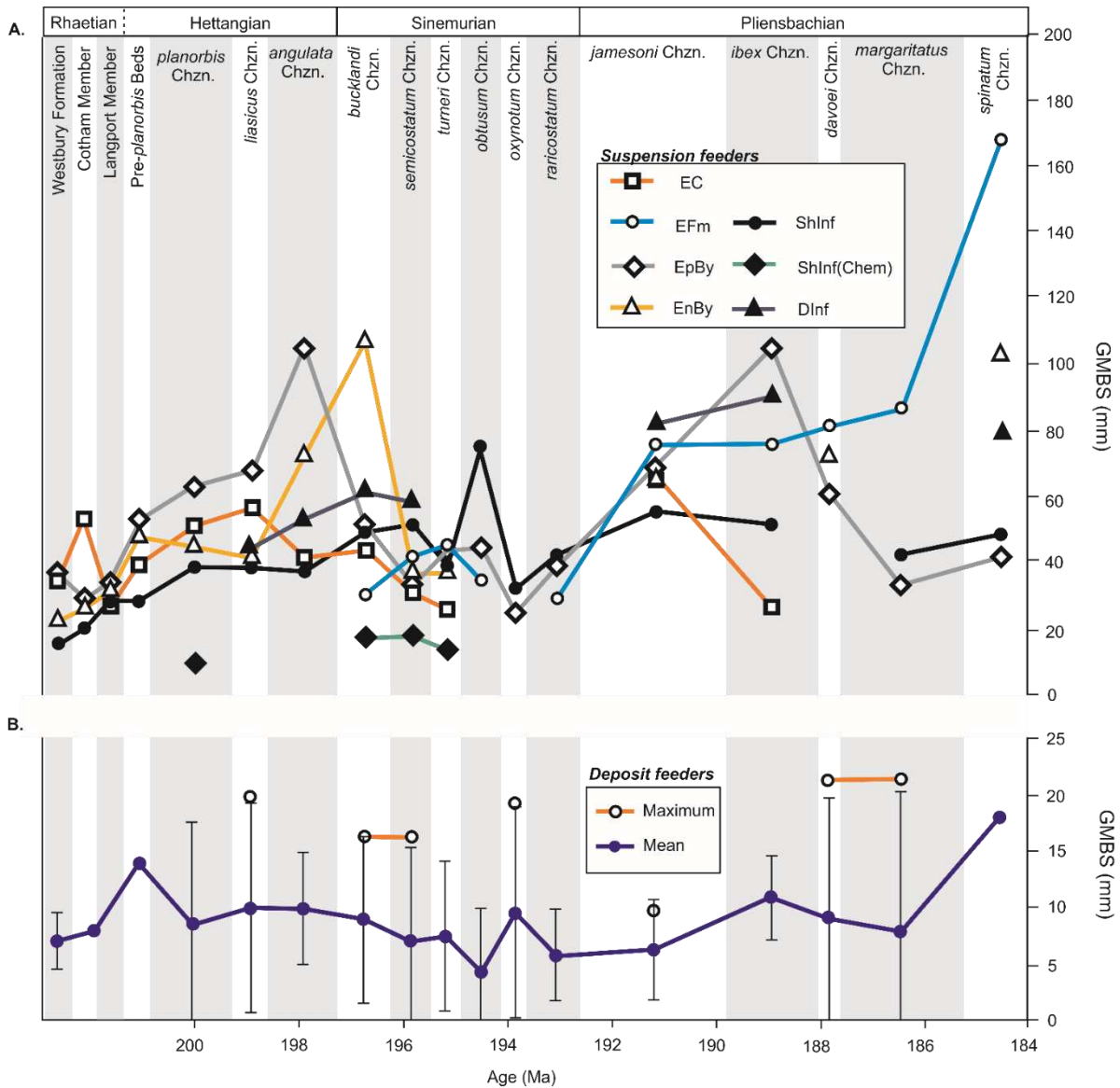
Fig. 6 Maximum GMBS for bivalves per ecological guild. A, Suspension feeding bivalves. Ecological abbreviations as follows: EC – epifaunal cemented; EFm – epifaunal facultative motile; EpBy – epibyssate; EnBy – endobyssate; ShInf – shallow infaunal; ShInf(Chem) – shallow infaunal with chemosymbionts (primarily represented by Lucinola limbata Terquem & Piette); DInf – deep infaunal. B, Deposit feeding bivalves; see Fig. 4 caption for details.

407

408   4.4 Within lineage trends

409   A subset of the 147 bivalve species studied herein have sufficient occurrence

410   data to examine both intraspecific and lineage size trends. For a full species-by-

411   species account see supplementary appendix 2.

412   Pseudopecten (Pseudopecten) equivalvis J. Sowerby remains small in both

413   mean and maximum size throughout the Hettangian and Sinemurian, only to

414   increase dramatically in size during the Pliensbachian (Fig. 7A). There are three

415   pulses of size increase: the first is between the raricostatum and jamesoni

416   chronozones when there is a doubling in mean and 133% increase in maximum. The

417   next is only reflected in the mean with a 90% increase from the jamesoni to ibex

418   chronozones. And, lastly a 68% increase in mean size from the margaritatus to the

419   spinatum Chronozone and 94% increase in the maximum. Overall from the

420   semicostatum to spinatum chronozones there is an increase of 254% in mean and

421   476% increase in maximum. There are however also phases of size reduction,

422   between the semicostatum and the raricostatum there is a decrease in mean by 37%

423   although maximum stays around the same (2% decrease).

424   The size trend in P. (P.) equivalvis predominantly reflects changes within the

425   Cleveland Basin, although there is a similar but more subdued size change in the

426   Hebrides Basin around the Sinemurian and Pliensbachian and in both basins the

427   giants were found in the spinatum Chronozone. The size increase is independent of

428   lithology: initially small individuals are from the semicostatum Chronozone oolitic

429   ironstone facies – the Frodingham Ironstone Member – whilst the raricostatum and

430   jamesoni size increase in the Cleveland Basin occurs within mudstones and the

431   margaritatus to spinatum increase is within ironstones again. Museum and field

432   collections show the same trend for this species, although for the oxynotum and

433   raricostatum chronozones the largest specimens are found in museum collections.

434

435   Entolium (Entolium) lunare Roemer increases between the bucklandi and

436   semicostatum-turneri chronozones by 46% in mean size, 51% in maximum (p

437   <0.001, Fig. 7B). This is however only temporary with mean size decreasing in the

438   subsequent chronozone by 29%, thereby returning the mean size to approximately

439   19 mm. The maximum size reflects the trends in the mean. Specimens are scarce

440   thereafter until the jamesoni Chronozone, when the largest mean and maximum

441   sizes were attained. The next time bin with >10 specimens is the margaritatus

442   Chronozone. At this interval the maximum size is 50% larger than that during the

443   early Sinemurian. Museum and field collections seldom have large numbers of E.

444   (E.) lunare from the same time, but nonetheless the trends in each collection are the

445   same. The semicostatum-turneri chronozone is the only zone that has a large

446   sample size in both collections, the museum specimens are however 43% larger

447   than the field collections.

448
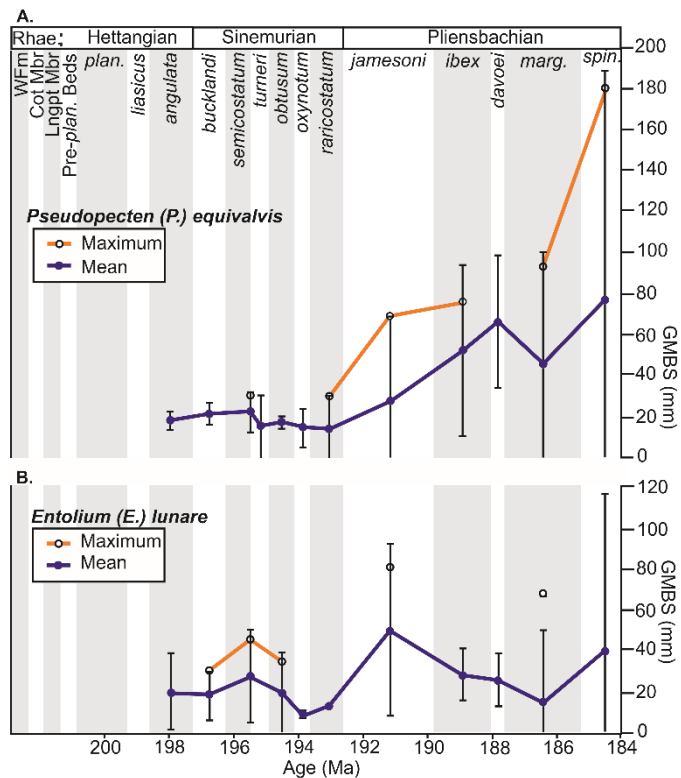
Fig. 7 Time-binned GMBS plot for A, Pseudopecten (P.) equivalvis and B, Entolium (E.) lunare. See Fig.4 caption for details, time bin abbreviations as follows: WFm – Westbury Formation; Cot Mbr – Cotham Member; Lngpt Mbr – Langport Member; Pre-plan. Beds – Pre-planorbis Beds; plan. – planorbis Chronozone; marg. – margaritatus Chronozone; spin. – spinatum Chronozone.

Chlamys (Chlamys) valoniensis (Defrance) is one of the few common species to survive the end-Triassic mass extinction in the study region. Initially very common in the Westbury Formation, and a basal shell bed of the Cotham Member, it is then absent from the remaining Cotham, before reoccurring in the Langport Member and is abundant again in the planorbis Chronozone. Specimens are plentiful from the Sutton Stone, a marginal/coastal facies. From the Westbury to Cotham mean body size declines by 10%. The communities of the planorbis Chronozone are 16% smaller than the Westbury and 7% smaller than the Cotham (Fig. 8), but only the former is a significant change ($p < 0.05$). The liasicus Chronozone populations from

463   marginal facies are significantly larger than those from the offshore Blue Lias

464   planorbis Chronozone (75%, p < 0.001).

465   Due to the bountiful supply of specimens from the Westbury Formation

466   variation between locations and collection styles can be tested for. The sizes are

467   broadly consistent between locations, albeit with a slight northwards size increase:

468   Somerset 26.1 mm, Glamorgan 27.2 mm, Aust 30.5 mm and Larne 34.0 mm. Both

469   field and museum collections show comparable sizes.

470
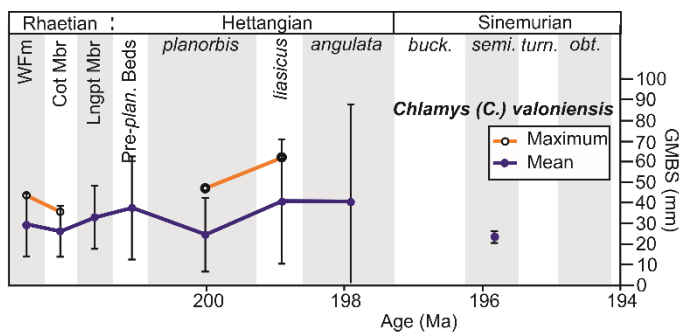
Fig. 8 Time-binned GMBS plot for Chlamys (C.) valoniensis. See Fig. 4 caption for details. Time bin abbreviations as follows: WFm – Westbury Formation; Cot Mbr – Cotham Member; Lngpt Mbr. – Langport Member; buck. – bucklandi Chronozone; semi. – semicostatum Chronozone; turn. – turneri Chronozone; obt. – obtusum Chronozone.

476   Camptonectes body size trends are here reported at the generic level as

477   many specimens were not preserved with shell material, which contains the

478   diagnostic ornament for species determination. This genus occurs commonly

479   throughout the Lower Jurassic and its size trends are somewhat out of kilter with the

480   overall Hettangian/earliest Sinemurian size patterns: maximum size progressively

481   declining from the planorbis to angulata Chronozone by 19% before increasing into

482   the semicostatum-turneri chronozones by 37% (Fig. 9A). Mean body size is broadly

483   similar showing a dip in the angulata Chronozone. Use of K-S tests defines three

484   intervals of significant size changes, the 20% (p = 0.002) decrease between the

485   semicostatum-turneri and obtusum chronozones. This initiates a period of reduced

486   body size within Camptonectes which is ended by a 38% (p = 0.002) increase

487   between the raricostatum and jamesoni chronozones. During the Pliensbachian

488   there is again a period of reduced body size there being a 28% decline between the

489   jamesoni and davoei chronozones.

490

491   Two main species of Oxytoma (Oxytoma) occur: O. (O.) fallax (Pflücker) and

492   O. (O.) inequivalvis (J. Sowerby). The former is present in Rhaetic-aged strata and

493   measurements are based entirely on museum collections, in most instances these

494   were shell-covered slabs. There is an increase of 49% in the maximum size between

495   the Cotham and the Langport members though only a slight but significant change in

496   the mean (increase by 10%, p <0.001). O. (O.) inequivalvis is typically larger than its

497   predecessor, O. (O.) fallax, and is well-represented in our dataset from the angulata

498   Chronozone to semicostatum-turneri Chronozone, although it has a greater

499   stratigraphic range. This species shows an increase in both the mean and maximum

500   size, expressed best in the maximum size however (Fig. 9B). From the angulata

501   Chronozone to the jamesoni Chronozone maximum size increases by 107%, slightly

502   declining by 9% during the davoei Chronozone.

503
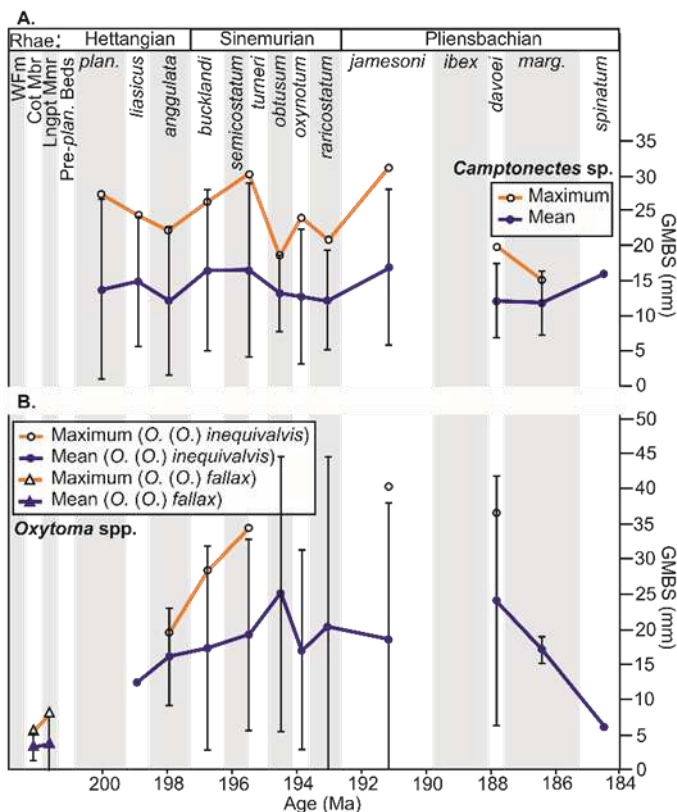
Fig. 9 Time-binned GMBS plot for A, species of Camptonectes and B, species of Oxytoma, see in-figure legend for induvial species present. See Fig.4 caption for details, time bin abbreviations as in Fig. 7.

Two species of Semuridia were recorded from the Lower Lias, S. obliqua Melville and S. quadrata Melville, size data for these are discussed here at the generic level owning to uncertainty regarding the validity of the two taxa, however most specimens bear a close resemblance to S. obliqua. Semuridia was first encountered within a 2 m thick blue-grey shale bed, associated with abundant Psiloceras ammonites. Specimens are common (n. 56) with the largest individual attaining a GMBS of 34.0 mm from this bed. During the liasicus Chronozone, specimens were found pyritised in a black shale associated with drift wood from St Audrie's Bay. Both mean and maximum body size is reduced at this point by 36%

517 and 27% respectively (p < 0.05). The angulata Chronozone specimens were

518 collected from a single shale bed in Pinhay Bay. Maximum size decreased while

519 mean size increased slightly by 13%.

520

521   Parainoceramya ventricosus (J. de C. Sowerby) is here recorded from

522 semicostatum to margaritatus chronozones. Greatest sizes occur in the ibex

523 Chronozone when maximum size attains 109.0 mm. There does not appear be any

524 directional trends within this species, merely appearing in the British Lias as an

525 already large species.

526

527   Analysis for Liostrea was only conducted at the generic level owing to the

528 plasticity of oyster morphology, and care was taken to avoid measuring forms of

529 Gryphaea with large attachment areas that can be confused for Liostrea. The genus

530 is well-represented with 379 specimens measured from the Westbury Formation to

531 the jamesoni Chronozone. They first appear in any significant numbers in the

532 Langport Member, becoming very abundant in the lower to middle Pre-planorbis

533 Beds. Mean body size remains fairly constant for the Hettangian between 18.8- 20

534 mm (Fig. 10A). Maximum size increases almost smoothly from the Langport to the

535 bucklandi Chronozone, with a total increase of 49% before declining in the

536 semicostatum Chronozone.

537   For the liasicus, angulata and bucklandi chronozones there is a good

538 relationship between host lithology in the Blue Lias Formation and body size: the

539 darker the lithology the smaller the bivalve. In the Pre-planorbis Beds specimens

540 come from laminated limestones and share similar body sizes to those from shales.

541   Museum and field collections show a good correspondence until the angulata and

542   bucklandi chronozones when field collections show a declining mean size.

543

544   Atreta intusstriata (Emmrich) is common in the Langport Member (n. 57), and

545   in the angulata Chronozone (n. 23). Between these two time bins there is a 26%

546   decline in mean body size, mirrored by a 25% decline in the maximum ($p < 0.001$,

547   Fig. 10B). Body size increases thereafter into the bucklandi Chronozone (mean by

548   21%, this time not a significant change $p = 0.38$) and does not regain the shell sizes

549   of the Langport community being still 10% smaller. The reduction in body size

550   between the Rhaetian and Hettangian is accompanied by a change in attachment

551   style. The Langport communities were by-and-large found as independent entities,

552   cementing, presumably to a firm substrate, whereas specimens from the Blue Lias

553   Formation were attached to larger shells, typically Plagiostoma giganteum or

554   Gryphaea (G.) arcuata Lamarck.

555
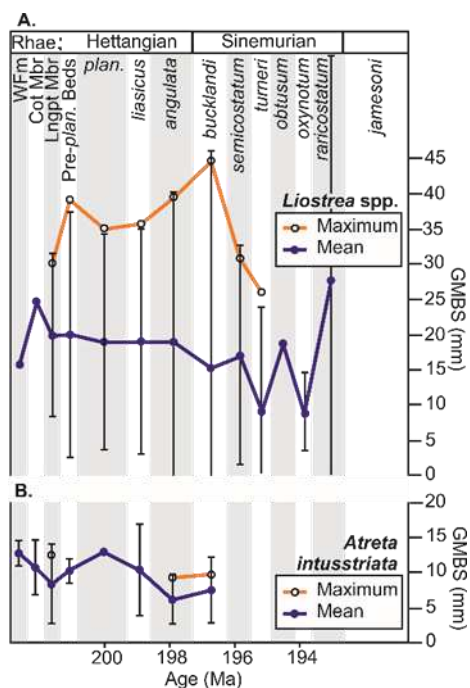
Fig. 10 Time-binned GMBS plot for A, undifferentiated of species of Liostrea and B, Atreta intusstriata. See Fig.4 caption for details and Fig. 7 for time bin abbreviations.

Two species of Modiolus have sufficient sample sizes to report within-species changes: - M. (Cyranus) hillanus (J. Sowerby) and M. (Modiolus) minimus (J. Sowerby). The former has a fairly constant maximum size, being around 30 mm in all time bins (Fig. 11A). The exception to this being for the Cotham Member, where both mean and maximum size decrease (59% and 67% respectively, p <0.001). The Langport Member specimens increase in size, to an average size 33% larger than the Westbury Formation. Mean body size is reduced in the planorbis Chronozone, down by 22% from the Langport Member.

M. (M.) minimus increases in abundance from the Langport Member to the planorbis Chronozone and decreases in size over this same interval (mean size by 54% and maximum by 56%, Fig. 11B), and remain small until the angulata Chronozone when their mean size increases insignificantly (11%, p = 0.2). There is no relationship between the size of a specimen and its host lithology. Museum and field collections show the same temporal trend in body size.

573
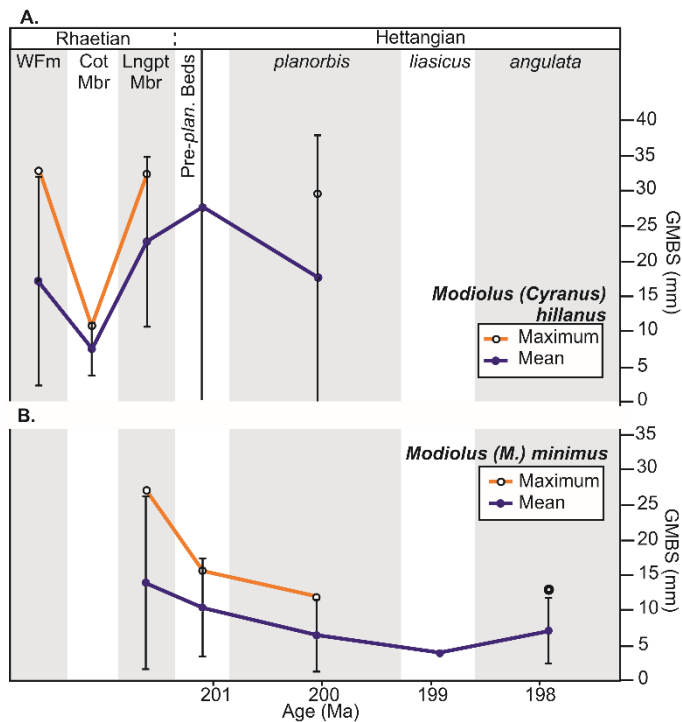
Fig. 11 Time-binned GMBS plot for species of Modiolus. A, M. (Cyranus)
hillanus and B, M. (M.) minimus. See Fig.4 caption for details and Fig. 7 for
time bin abbreviations.

Pteromya crowcombeia Moore is one of the few species to remain reasonably common across the end-Triassic crisis, it ranges from the Penarth Group to planorbis Chronozone. Mean body size decreases in the Cotham Member by 28% accompanied by a 24% decline in maximum size (p = 0.02; Fig. 12A). This is a brief decrease in size which is succeeded by an increase of 53% in mean and 111% in maximum size during the Langport Member. The trend continues in the Pre-planorbis interval, with mean body size rising by a further 43%.

Isocyprina (Eotrapezium) ewaldi (Bornemann) is abundant in the Westbury Formation, forming shell pavements. From sections in Northern Ireland, bed-by-bed sampling shows this species increases in size through the Westbury Formation. This

588   trend is sustained into the Cotham Member, when using the time-binned approach,

589   with mean size increasing by 24% (Fig. 12B). There is however a marked reduction

590   in sample size at this time because it fell victim to the end-Triassic mass extinction.

591

592   Neocrassina (Neocrassina) gueuxii (d'Orbigny) undergoes an extraordinary

593   increase in body size between the planorbis and liasicus chronozones of 215% (Fig.

594   12C). This is followed by a slight decline into the angulata Chronozone, but

595   maximum size continues to increase resulting in an overall 283% increase in

596   maximum size between the planorbis to the angulata chronozones. The mean and

597   maximum size then decrease in the semicostatum-turneri Chronozone by 24% and

598   12% ($p < 0.05$) respectively.
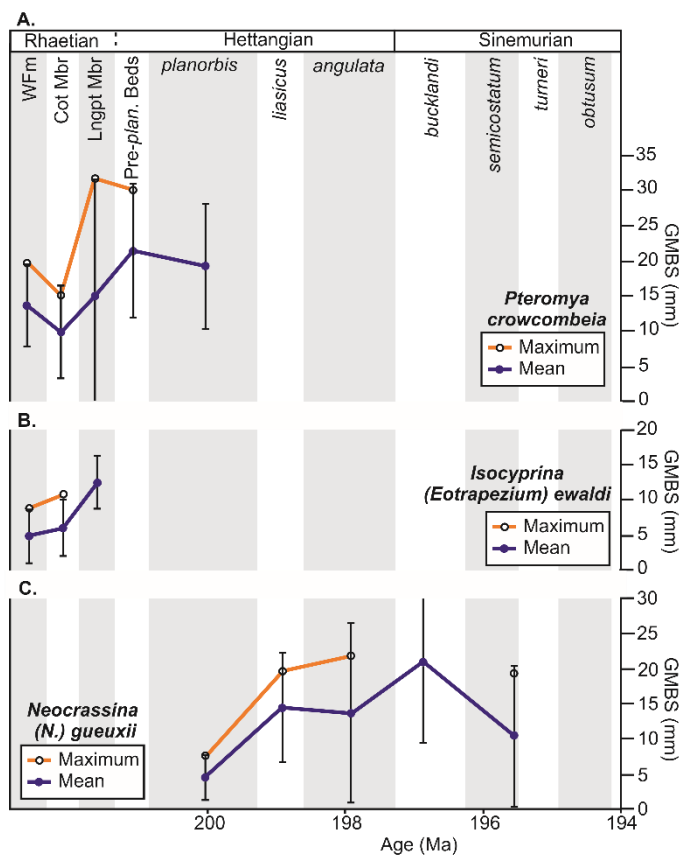
599

600 **Fig. 12 Time-binned GMBS plot for A, Pteromya crowcombeia, B, Isocyprina**

601 **(Eotrapezium) ewaldi, C Neocrassina (N.) gueuxii. See Fig.4 caption for details,**

602 **time bin abbreviations as in Fig. 7.**

603   Cardinia ovalis (Stutchbury) survived the end-Triassic mass extinction event.

604 Size plot shows two distinct size classes, smaller individuals from the Penarth Group

605 and consistently larger ones from the Hettangian (Fig. 13A). Each population shows

606 little in the way of size variation but a single stepped increase in size between the

607 two with mean and maximum increasing by 75% and 67% respectively, between the

608 Cotham Member and planorbis Chronozone. Growth line analyses show the Cotham

609 specimens have fewer and more closely spaced primary growth lines than those of

610 the Blue Lias and Waterloo Mudstone formations (Fig. 13B).

611   C. ovalis is common in the planorbis Chronozone of Northern Ireland, and the

612 liasicus Chronozone elsewhere in Britain. In the latter chronozone, samples from

613 Glamorgan have the largest average, followed by those from Mochras and smallest

614 being of the Somerset coast indicating a likely offshore decreasing size trend. In all

615 the time bins with sufficient material, museum and field collections have a

616 comparable mean size.

617   Cardinia ovalis is replaced by Cardinia listeri (J. Sowerby) in the Sinemurian,

618 with a bucklandi Chronozone maximum size 47% larger than its predecessor.
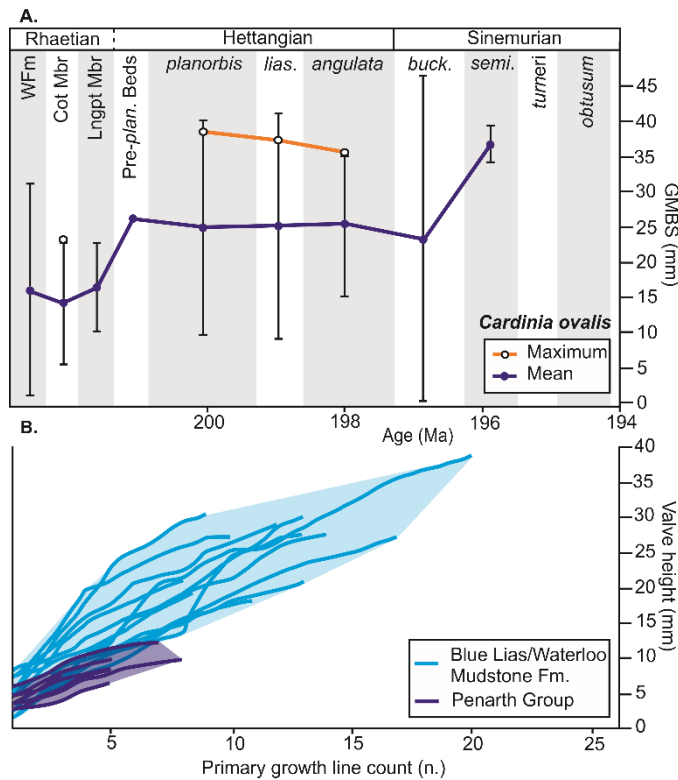
Fig. 13 A, Time-binned GMBS plot for Cardinia ovalis, see Fig.4 caption for details, time bin abbreviations: WFm – Westbury Formation; Cot Mbr – Cotham Member; Lngpt Mbr – Langport Member; lias – liasicus Chronozone; buck. – bucklandi Chronozone; semi. – semicostatum Chronozone. B, Primary growth line plot for C. ovalis specimens from the Penarth Group and Blue Lias/Waterloo Mudstone formations.

Mactromya cardioideum (Phillips) shows mean and maximum body size fluctuations in the Hettangian and early Sinemurian but without any long-term trends over that time. Subsequently, there is a 54% (p <0.001) increase in mean size from the semicostatum Chronozone to the ibex Chronozone (Fig. 14A). The larger specimens, from the Blockley Quarry site in the Severn Basin, have more growth lines than their Blue Lias predecessor (Fig. 14B) indicating they achieved their greater size due to increased longevity.
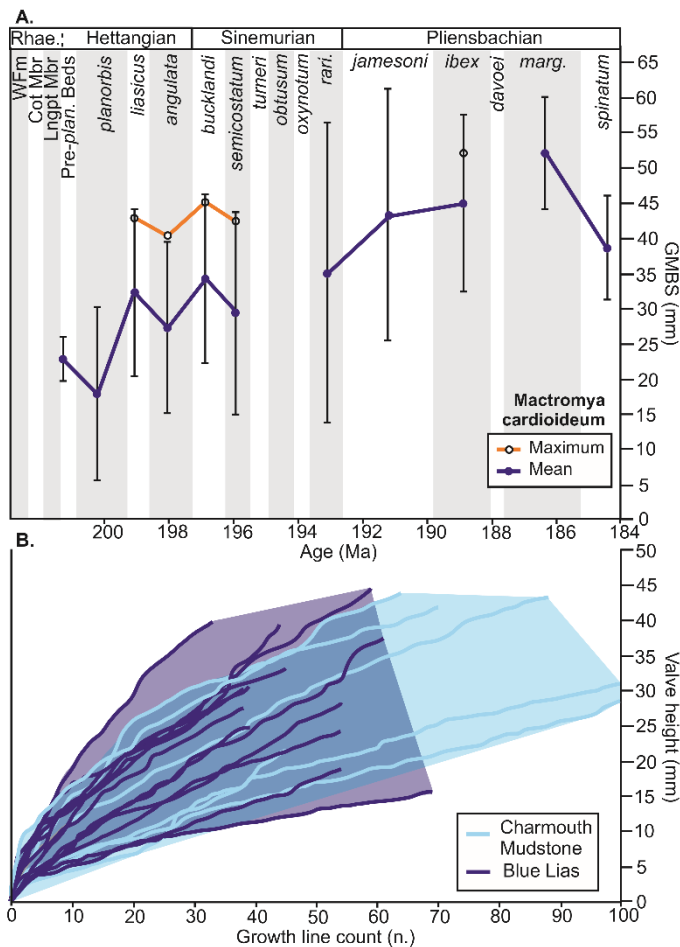
Fig. 14 A, Time-binned GMBS plot for Mactromya cardioideum, see Fig.4 caption for details, time bin abbreviations as in Fig. 7 with addition of rari. – raricostatum Chronozone. B, Growth line plot also for M. cardioideum specimens from the Blue Lias Formation and from Blockley Quarry, Severn Basin (Charmouth Mudstone Formation).

Four species of Protocardia (Protocardia) are present in the study interval and show minimal range overlap (Fig. 15). P. (P.) rhaetica (Merian) is abundantly recorded in the Westbury Formation before going extinct in the lower Cotham Member. There is no change in the mean nor the range of sizes. P. (P.) philippianum (Dunker) appears in the aftermath of the end-Triassic mass extinction and is plentiful in the Langport Member and Pre-planorbis Beds but dwindles in abundance rapidly

645   thereafter. Between the Langport Member and Pre-planorbis Beds there is no

646   significant size change (p > 0.05) but the rarely occurring, geologically youngest

647   individuals are far smaller, being around one third the size of those from the Pre-

648   planorbis Beds. The next Protocardia species – P. (P.) oxynoti (Quenstedt) is also

649   the smallest species, and was here found to range from the bucklandi to

650   raricostatum chronozones. It is common in the Mochras core from the semicostatum

651   to turneri chronozones and at Robin Hood's Bay from the turneri to raricostatum

652   Chronozone but there is little change in size except in the oxynotum Chronozone

653   where specimens are slightly smaller. P. (P.) truncata (J. de C. Sowerby) is the

654   geologically youngest and largest species encountered in this study, and is common

655   only in the margaritatus and spinatum chronozones, especially in the Staithes

656   Sandstone and the Marlstone Rock formations. These were measured from museum

657   collections with few from direct field observations. Between the margaritatus

658   Chronozone and the spinatum Chronozone there is a 20% (p <0.001) decrease in

659   the mean whilst maximum is broadly similar.
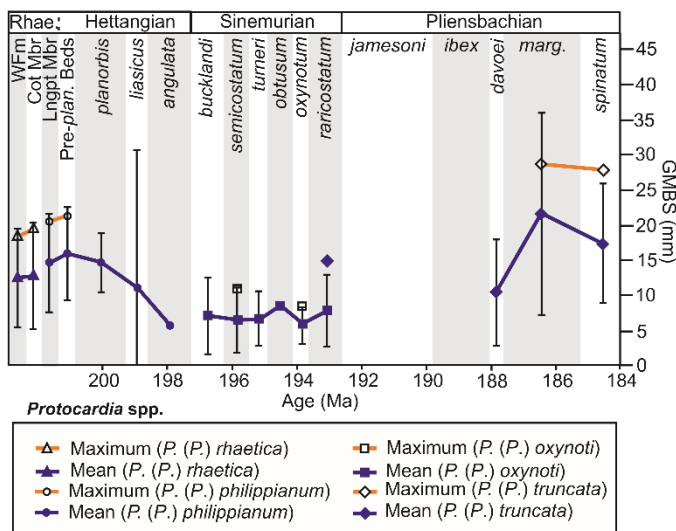
660

661 **Fig. 15 Time-binned GMBS plot for species of Protocardia (Protocardia), see**

662 **figure legend for species details, and also see figure captions for Figs. 4 and 7**

663 **for details of error bars and abbreviations.**

664   Gresslya galathea (Agassiz) occurs during the Hettangian and early

665 Sinemurian but samples are almost entirely restricted to Glamorgan. This species

666 shows a single stepped increase in size between the liasicus and angulata

667 chronozones (30% mean, 58% max, Fig. 16A). Thereafter, mean body size is fairly

668 consistent. G. galathea is followed by the far larger G. intermedius (Simpson), which

669 has an average size of 40 mm compared to 20 mm of its predecessor, this species is

670 primarily seen in the margaritatus and spinatum chronozones.

671

672   Pleuromya striatula Agassiz first occurs (rarely) in the Pre-planorbis Bed

673 becoming more abundant in the angulata and bucklandi chronozones, with an

674 insignificant ($p > 0.05$) increase in mean and maximum size of around 10%. P.

675 striatula is considered the ancestor of P. costata (Young & Bird), which has a first

676 questionable appearance in the semicostatum Chronozone (n. 3). There are

677 however only two times when the species is sufficiently abundant to make comment

678 on any size trends: ibex and spinatum chronozones when mean sizes are 32.5 mm

679 and 33.6 mm respectively. There is however quite a marked increase (43%) in the

680 maximum size 38.3 mm to 54.6 mm (Fig. 16B).

681

682   Two main species of Pholadomya (Pholadomya) were recorded in this study,

683 P. (P.) glabra Agassiz and P. (P.) ambigua J. Sowerby (a single specimen of P. (P.)

684 "ovalis" was also measured from the ibex Chronozone). P. (P.) glabra is chiefly

685   recorded from Glamorgan and has a mean body size around 30 mm which increases

686   from the liasicus Chronozone to the bucklandi Chronozone by 62%, accompanied by

687   a 41% increase in the maximum size (Fig. 16C). Between the angulata and

688   bucklandi chronozones there is a 36% increase in size which may be attributable to

689   an increase in growth rate and longevity. This is suggested by several of the

690   bucklandi specimens which attain a larger size for the same number of growth lines,

691   and continued to grow thereafter, thereby also show a greater number of growth

692   lines (Fig. 16D). P (P.) glabra is replaced by P. (P.) ambigua during the late

693   Sinemurian. This later species shows little in the way of a with-species size change

694   with an 8% increase in the mean and a 15% in the maximum size between the ibex

695   and spinatum chronozones ($p > 0.05$). P. (P.) ambigua does however form part of a

696   long-term generic body size increase. Between the mean sizes of P. (P.) glabra in

697   the liasicus Chronozone to the mean size of P. (P.) ambigua during the spinatum

698   Chronozone there is a doubling of size.
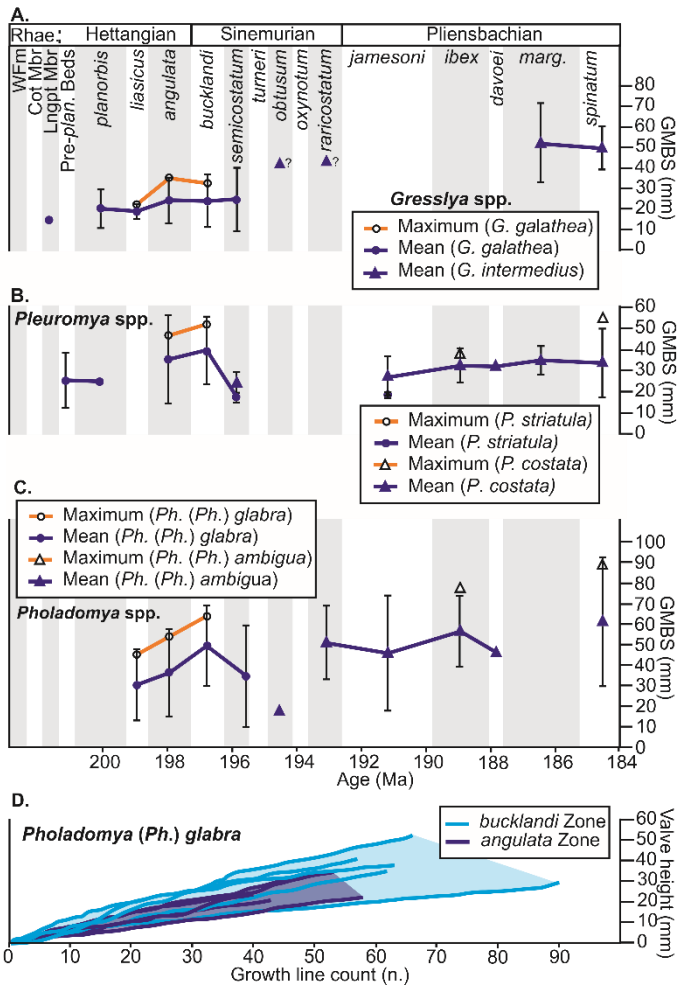
Fig. 16 Time-binned GMBS plot for A, species of Gresslya, B, species of Pleuromya, and C, species of Pholadomya (Pholadomya), see subfigure legends for individual species featured. See Fig.4 caption for details and Fig. 7 for time bin abbreviations. D, Growth line plot for P. (Ph.) glabra from the Blue Lias Formation comparing specimens of the angulata and bucklandi chronozones.

5. Discussion

5.1 Body size trends

5.1.1 Lilliputians

710   Of the 26 species discussed in detail there are only six species that survived

711   the mass extinction and have sufficient data to assess size trends. Of these, two

712   species could be considered to exhibit the Lilliput Effect: Modiolus (Cyranus) hillanus

713   and Pteromya crowcombeia, and possibly two others: Chlamys (C.) valoniensis and

714   Cardinia ovalis. In M. (Cyranus) hillanus and P. crowcombeia pre-extinction body

715   sizes were restored by the Langport Member, less than 0.15 Myr after the extinction.

716   It is questionable if C. (C.) valoniensis is an example of the Lilliput Effect because is

717   very rare post extinction it making it difficult to judge its size. It was not common

718   again until 2.3 Myr after the extinction, in the liasicus Chronozone, when it had re-

719   attained its pre-extinction size. Cardina ovalis also cannot unequivocally be shown to

720   have a Lilliput trend, because the species is poorly known/very rare prior to the

721   extinction interval. During the Cotham Member (the extinction interval) C. ovalis is

722   small with specimens having few, closely spaced growth lines when compared to the

723   Hettangian when this species is bigger and has more growth lines that are typically

724   spaced at wider intervals. In summary, despite claims that the Lilliput Effect was

725   common during the end-Triassic mass extinction (Barras and Twitchett, 2007;

726   Clémence and Hart, 2013; Mander et al., 2008), it can only be clearly demonstrated

727   to have occurred for two species.

728

729   5.1.2 Brobdingnagians

730   Alongside Plagiostoma giganteum, Atkinson et al. (2019) reported the

731   Brobdingnag Effect in two other species of limid bivalves, here a further five species

732   of bivalve exhibit a clear Brobdingnag trend in the aftermath of the mass extinction:

733   Lucinola limbata Terquem & Piette, Neocrassina (N.) gueuxii, Oxytoma (O.)

734   inequivalvis, Gresslya galathea and Pholadomya (Ph.) glabra. These all exhibit a

735   size increase over a similar interval of time to that of P. giganteum. From growth

736   lines analysis of P. giganteum it was found that the size increase reflected increased

737   growth rates and to some extent a greater longevity (Atkinson et al., 2019), a similar

738   case in point is seen with Ph. (Ph.) glabra although there is a greater overlap in

739   growth rates between specimens measured from the angulata and bucklandi

740   chronozones. The bucklandi-aged specimens often have a greater number of growth

741   lines, here likely indicating an increased life span. Species of Liostrea may also show

742   a Brobdingnag trend as the genus exhibits increasing maximum size following the

743   mass extinction, however improved taxonomy is required to show this.

744   A further three species show a size increase over the span of the study

745   interval, Entolium (E.) lunare, Pseudopecten (P.) equivalvis and Mactromya

746   cardioideum. These three differ in having a delayed size increase that does not

747   begin until the Sinemurian or Pliensbachian, some 9 Myr after the end-Triassic mass

748   extinction. The size increase of M. cardioideum was driven solely by greater

749   longevity as the larger Pliensbachian specimens have similar growth line spacing but

750   more growth lines than those in the Hettangian/earliest Sinemurian.

751   The Brobdingnag Effect was a significant feature in the aftermath of the end-

752   Triassic mass extinction and was still important 17 Myr later, at the end of the

753   Pliensbachian Stage. The generally large size of bivalves in the spinatum

754   Chronozone was caused by the culmination of long-term size increase trends

755   amongst species that appeared earlier. The average size of newly arriving bivalves

756   does not feature a size increase for this time (Fig. 4B).

757

758   5.1.3 Cope*'s Rule*

759   The role of Cope's Rule during the Hettangian and Pliensbachian phases of

760   size increase is hard to assess accurately as the ancestry of the new species is not

761   always clear. If assumptions are made that a geologically younger species is the

762   descendant of a geologically older species of the same genus (in cases where there

763   are multiple potential ancestors the most morphologically similar is chosen) then size

764   changes between these can be assessed. As demonstrated above, the Hettangian

765   size increase is facilitated by both the appearance of increasingly large new taxa and

766   also larger new species of pre-existing genera. However, when broken down further

767   there are as many instances of new species of a lineage being smaller than their

768   potential ancestor as there are those that display a Cope's Rule pattern. The

769   succession of species within the genera Gresslya, Pholadomya, Oxytoma and also

770   Cardinia show perhaps the best candidates for Cope's Rule. Although insufficient

771   material was measured during this study, Hodges (2000) also found an increase in

772   size between Dacryomya heberti (Martin) and D. gaveyi Cox between the

773   Sinemurian and Pliensbachian, a size trajectory that appears to have been sustained

774   in to the Toarcian with D. ovum (J. de C. Sowerby) (Caswell and Dawn, 2019).

775   This therefore suggests that Cope's Rule did play a role in the size increase in

776   the Lower Jurassic, but the Brobdingnag Effect is more crucial to explain the large

777   bivalves of the spinatum Chronozone.

778

779   5.1.4 No trends

780   Not all bivalves show a size trend in the Lower Jurassic. Some simply do not

781   alter their size (either significantly or with any distinct direction) across the duration of

782   the study. Examples of this include most species of protobranchs and

783 Parainoceramya ventricosus. Camptonectes size fluctuates during the Lower

784 Jurassic, but only shows a distinct pattern during the Sinemurian, when they show a

785 size reduction.

786

787 5.1.5 Those that get smaller

788   Alongside the previously reported Plagiostoma punctatum J. Sowerby

789 (Atkinson et al., 2019), there are three cases of bivalves reducing in size over the

790 same interval that others show a Brobdingnag trend. These are Semuridia sp., Atreta

791 intusstriata and Modiolus (M.) minimus. These inverse-Brobdingnags are not

792 Lilliputians because they exhibit a progressive reduction in body size during the

793 recovery.

794   The Sinemurian is marked by a general suppression of body size in the

795 bivalves (excluding the obtusum Chronozone; Fig. 4A); a phase herein referred to as

796 the Sinemurian Small Episode (SSE). The lowest point of the SSE is in the oxynotum

797 Chronozone when the data are all from the Cleveland Basin. Although this particular

798 basin hosts bivalves that are usually smaller than most other basins until the

799 Pliensbachian, the SSE is not merely an artefact of the relative contribution of

800 material measured from each basin because the SSE in the Cleveland Basin is

801 bracketed by comparably larger bivalves in the bucklandi and jamesoni

802 chronozones. The Mendips, EMS, Dorset and Bristol Channel Basin all show the

803 SSE where it is primarily expressed as an initial size reduction following the angulata

804 Chronozone size peak. Plagiostoma giganteum also shows a decrease in body size

805 at this time (Atkinson et al., 2019).

806   Other taxa that show concurrent size reductions are: Cardinia listeri,

807   Neocrassina (N.) gueuxii, Camptonectes and Liostrea. The SSE is expressed not

808   only as an intraspecific size reduction but also, those species that originate during

809   this interval are smaller compared to those that originated in the angulata

810   Chronozone. Thus, Entolium (E.) lunare and Pseudopecten (P.) equivalvis both

811   originate at small body sizes during this interval and increase in size during the

812   Pliensbachian. Additionally, new species of Protocardia and Modiolus are smaller

813   than their Hettangian predecessors.

814

815   5.1.6 Gryphaea

816   The evolutionary lineage of the oyster Gryphaea (Gryphaea (G.) arcuata - G.

817   (G.) mccullochi J. de C. Sowerby – G. (G.) gigantea J. de C. Sowerby) has been

818   widely reported (Hallam, 1975, 1968; Johnson, 1994; Jones and Gould, 1999; Nori

819   and Lathuiliére, 2003). G. (G.) arcuata first appeared in the angulata Chronozone

820   and increases in size into the bucklandi Chronozone before decreasing in the

821   semicostatum Chronozone (Johnson, 1994). It is then replaced by the G. (G.)

822   mccullochi which is larger than the youngest G. (G.) arcuata specimens but does not

823   exceed the sizes of Gryphaea in the bucklandi Chronozone. Ironically, G. (G.)

824   gigantea first appears at a smaller size than is predecessor: G. (G.) mccullochi,

825   before increasing in size from the upper jamesoni Chronozone onwards (Johnson,

826   1994). The angulata – bucklandi Chronozone size increase and subsequent

827   reduction during the semicostatum Chronozone seen within G. (G.) arcuata matches

828   that seen in other bivalve species featured in this study. There is a paucity of

829   measured Gryphaea samples from the interval of the SSE with the only sample in

830   the obtusum Chronozone.

831

5.1.7 Bivalve size changes across Europe and beyond

No other studies have systematically documented body size changes during the Early Jurassic, but the available information suggest that the trends seen in British bivalves are repeated elsewhere. Johnson (1984) reported size changes within the Pectinidae and Propeamussidae and showed a size increase in Entolium (E.) lunare and Pseudopecten (P.) equivalvis in Germany, Camptonectes and Chlamys (Chlamys) textoria (Schlotheim) also show a size increase from the Sinemurian to upper Pliensbachian of Germany. Data for the Hettangian are very limited, only Hallam (1975) covers this interval albeit in scant detail: only the initial and final maximum size of a species is documented. Hallam measured bivalves from the collections of the British Museum (Natural History) that included collections from Germany and France, and found a Hettangian to Pliensbachian size increase indicating the trends occurred across the European shelf sea. Unfortunately there are no other size data available from other regions such as the Tethyan realm, although it is potentially noteworthy that sizes of Pliensbachian bivalves from Serbia are comparable to those reported here (Radulović 2013).

Panthalassic records of bivalves from the South America have received considerable attention (e.g. Aberhan, 1994; Damborenea, 1987a, 1987b; Damborenea et al., 2017), although temporal size data is mostly absent. Nonetheless, Damborenea's monographs (Damborenea, 2002, 1987a, 1987b) present some 240 measured specimens from Argentina at Stage resolution but with a dearth of Hettangian specimens. These indicate there is a size increase between the Sinemurian and the Pliensbachian at the community level.

855

856   5.1.8 Size trends in other groups

857   Body size trend studies of other marine invertebrates are restricted to the

858   well-known Liassic ammonites. Dommergues et al. (2002) provide a compendium of

859   ammonite shell volumes per chronozone that can be compared to our bivalve

860   maximum body sizes (Fig. 17). For the Hettangian and Sinemurian, the two datasets

861   are remarkably consistent, both bivalves and ammonites show increasing maximum

862   sizes through the Hettangian. Peak ammonite size is attained in the bucklandi

863   Chronozone, slightly later than the bivalves (although if Plagiostoma giganteum data

864   of Atkinson et al. (2019) are included with our data herein the two maxima coincide).

865   Ammonites also show a size trough (the SSE) for much of the Sinemurian and

866   feature a brief renewal of size increase in the obtusum Chronozone, just as bivalves

867   do. The SSE is ended in both datasets by an increase in size from the oxynotum to

868   the raricostatum Chronozone. The remarkable congruence of bivalve and ammonite

869   data disappears in the Pliensbachian when ammonite shell volume decreased whilst

870   the bivalves showed two further increases in size during the ibex and spinatum

871   chronozones.
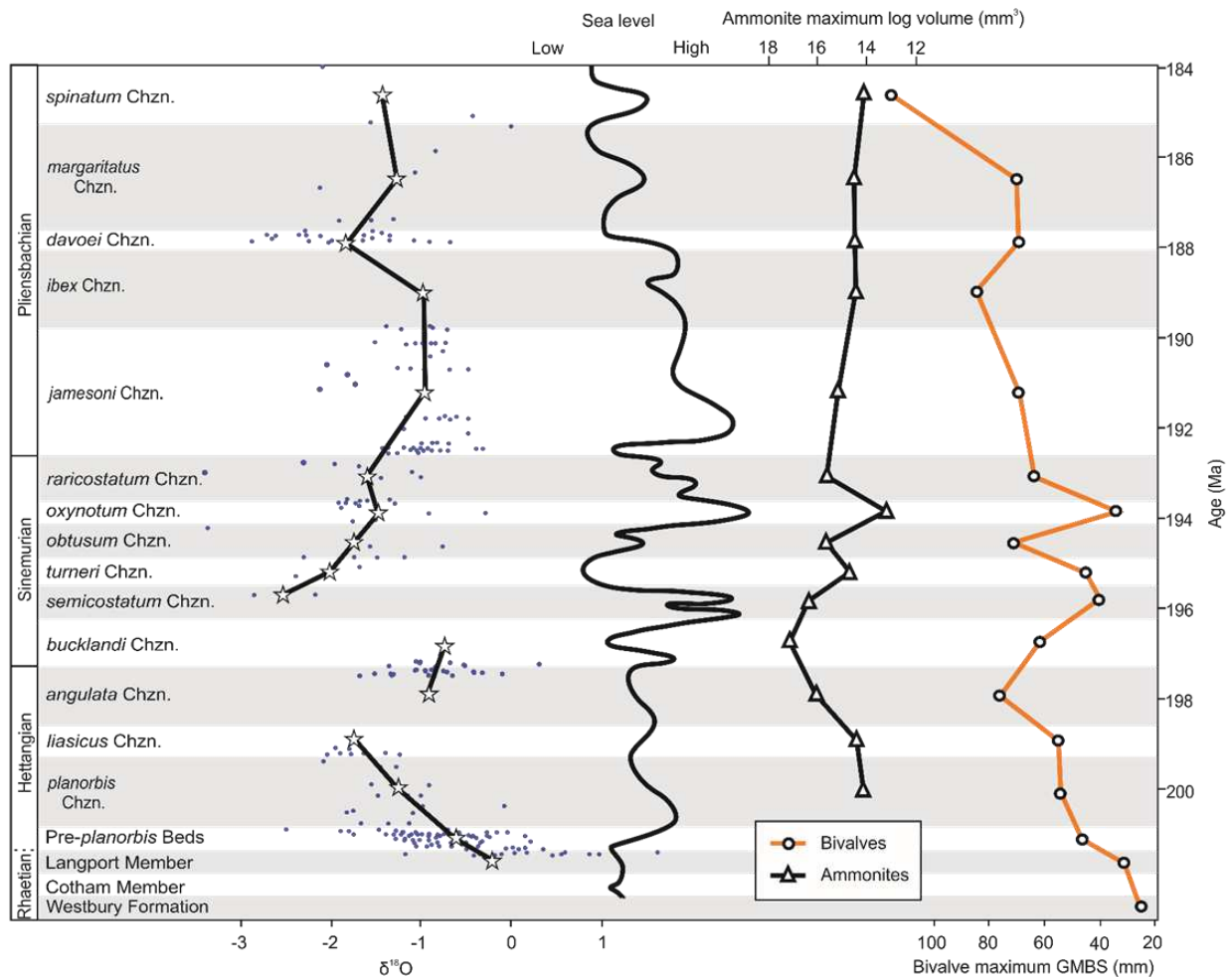
Fig. 17 Temperature and sea level changes in relation to maximum GMBS of all bivalves and maximum log volume of ammonites. δ¹⁸O isotope curve compiled from Korte et al. (2009); Korte and Hesselbo (2011); van de Schootbrugge et al. (2007); Weedon (1987). Hollow stars depict time bin average δ¹⁸O values. Sea level curve derived from Hesselbo (2008); Hesselbo and Jenkyns (1998) and Wignall and Bond (2008). Maximum GMBS of bivalves from this study and maximum log volume of ammonites per ammonite chronozone from Dommergues et al. (2002).

5.2 Possible causes of size change

5.2.1 Sea level, sediments and size

884   Three phases of size change occur amongst Rhaetian and Lower Jurassic

885   bivalves whereas there are four distinct phases of sedimentation in the British Isles.

886   The faunas of the Penarth Group lack any large bivalves, never exceeding 60 mm.

887   This has been attributed to abnormal salinities (Hallam and El Shaarawy, 1982;

888   Márquez-aliaga et al., 2010), as large bivalves are found elsewhere in normal marine

889   settings at this time (Hallam, 2002). The reduced body size seen in three species

890   during the extinction interval recorded in the Cotham Member could be linked to a

891   salinity control because this unit likely accumulated in hypersaline, brackish or even

892   freshwater conditions (Wignall and Bond, 2008), but other causes are considered

893   below.

894   Maximum size increases markedly from the Penarth Group to the Blue Lias

895   Formation and coincides with the development of normal marine conditions (Hallam

896   and El Shaarawy, 1982; Hesselbo et al., 2004). This change may have played a role

897   in bivalve size increase as demonstrated by Cardinia ovalis, which exhibited stunting

898   of growth and size during deposition of the Penarth Group but both improved during

899   the onset of fully marine conditions with no subsequent size change thereafter. The

900   change from the Lilstock to the Blue Lias Formation is also a change in substrate

901   consistency and this may explain the size reduction seen in Atreta intusstriata

902   because, during periods of firm substrate this species is found attached to the

903   seabed, something unachievable on soupy substrates when A. intusstriata could

904   attach only to other shells. This change is accompanied by a size reduction, perhaps

905   owing to limitations of space thus imposed.

906   For the remainder of the Hettangian, size increase occurs within the same

907   formation (the Blue Lias) whilst sea levels were fluctuating (Fig. 17). In itself these

908   sea level changes seem unlikely to have been responsible for the increased size

909   although bivalves generally decrease in size in deeper waters as shown by the

910   smaller average size of bivalves in deeper water setting of the Central Somerset

911   Basin. Oxygen deficiency was more prevalent in deeper waters, which may account

912   for the undersized nature of the bivalves there (Atkinson and Wignall, 2019). The

913   temporal size increase of bivalves in the Hettangian is superimposed on this

914   proximal-distal size trend and is not related to relative water depth changes.

915   The initiation of the SSE is largely coincident with deepening (Hesselbo,

916   2008), and so could represent a depth control on size. This is supported during the

917   turneri Chronozone when a brief shallowing is coincident with a temporary size

918   increase seen in both the Dorset and Cleveland basins. The total bivalve database

919   (Fig. 17) shows this size increase continues into the obtusum Chronozone but this is

920   only seen on the EMS and is likely an effect of the Frodingham Ironstone, discussed

921   below. The end of the SSE coincides with a lowering of sea levels. But this tenuous

922   link to sea level falls apart in the jamesoni Chronozone when there is a significant

923   deepening and no consequent size reduction.

924   It seems apt to here summarize the relationship between large body sizes and

925   ironstones. For the obtusum Chronozone the largest bivalves occur in the

926   Frodingham Ironstone Member and likewise the largest bivalves from the spinatum

927   Chronozone are mostly from ironstone facies. Such sediments are thought to have

928   accumulated slowly on seafloor highs or shoals (Hallam and Bradshaw, 1979). The

929   well-aerated, clear waters together with increased nutrient supply likely favoured

930   bivalve growth in such settings (Johnson, 1984; Nicol, 1967). However, there

931   remains a question over the size increase seen in Pseudopecten (P.) equivalvis and

932   Entolium (E.) lunare between the obtusum and spinatum chronozones, which

933   occurred within similar ironstone facies, suggesting some other influence at play.

934

5.2.2 Redox

The degree of oxygenation within the Hettangian and earliest Sinemurian of the British Isles has been assessed using pyrite framboid populations (Atkinson and Wignall, 2019). These record a considerable degree of oxygen restriction throughout the interval with no significant improvements or trends between the planorbis and bucklandi chronozones. Bivalve sizes increased at this time (Fig. 18), indicating there was little or no overall redox control. The deeper waters of the Central Somerset Basin do however show more frequent intense intervals of water column anoxia/dysoxia than seen in the shallower Glamorgan sections, which may account for the smaller size of bivalves measured in the former location.

945
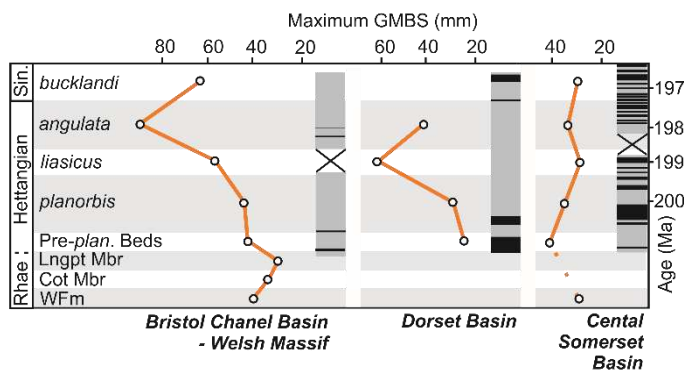
Fig. 18 Maximum GMBS trends for the Bristol Channel Basin-Welsh Massif, Dorset and Central Somerset basins and oxygenation states for each of the three basins from Atkinson and Wignall (2019). Hollow circles show maximum GMBS, from this study. Redox states are depicted as alternating grey and black bars, the former indicate periods with dysoxic/oxic framboid size distributions, black bars anoxic distributions, regions crossed out lack data. Time bin abbreviations same as Fig. 5. Time scaled to Weedon et al. (2019).

953

954   5.2.3 Temperature

955   The relationship between temperature and size is difficult to evaluate because

956   of a paucity of Lower Jurassic proxy data. The release of large volumes of

957   greenhouse gases during emplacement of the Central Atlantic Magmatic Province is

958   suggested to have caused intense global warming during the end-Triassic mass

959   extinction (Beerling and Berner, 2002). Evidence from decreasing leaf stomatal

960   density at the time suggests 3-4°C of atmospheric temperature increase across the

961   extinction interval (McElwain et al., 1999). Subsequent temperature fluctuations in

962   the Lower Jurassic are ill constrained, but the available data indicate no major

963   changes (Fig. 17). Korte et al. (2009) suggest sea-floor temperatures of between 7-

964   14°C for the upper Langport Member (and ostensibly a dramatic cooling from the

965   preceding hot conditions during Cotham deposition, presuming salinity has not

966   affected these results), rising to 12-22°C for the planorbis and lowermost liasicus

967   chronozones based on oxygen isotope ratios from oyster calcite. Oxygen isotope

968   data from the angulata and bucklandi chronozones indicate temperatures still within

969   this range (Weedon, 1987; Weedon et al., 2018), suggesting temperatures did not

970   drive the contemporaneous size increases.

971   The later Sinemurian to Pliensbachian has a more continuous oxygen isotope

972   record that indicates potentially warmer conditions (Korte and Hesselbo, 2011).

973   Temperature estimates for the semicostatum and turneri chronozones are 19-25°C,

974   however these progressively cool to values that are again similar to the Hettangian

975   (13-21°C, Korte & Hesselbo, 2011), again suggesting that temperature was no t the

976   cause of the SSE.

977   The patterns of size changes seen in the Pliensbachian are also unlikely to be

978   related to temperatures as no covariation is seen. Sizes increase in both mean and

979　maximum towards the ibex Chronozone, but temperature is poorly constrained at

980　this time (Fig. 17). The succeeding davoei Chronozone is considered a period of

981　brief warming (Dera et al., 2009; Gómez et al., 2016), prior to cooling in the latest

982　Pliensbachian (Bailey et al., 2003; Korte and Hesselbo, 2011; Rosales et al., 2004;

983　Suan et al., 2010) but bivalves show no significant body size change over this

984　interval.

985

986　5.2.4 Food availability

987　　　Food supply is a major factor affecting body size in modern marine molluscs

988　(Berke et al., 2013; Linse et al., 2006; Munroe et al., 2013; Olabarria and Thurston,

989　2003; Smith et al., 2008) and some authors use the size of bivalves as a proxy for

990　primary productivity (e.g. Vermeij 2011). To simply use a "size = productivity"

991　approach in this study would clearly be a case of circular reasoning. However, there

992　are other patterns that suggest improved food supply may have been a factor for the

993　size increase amongst Lower Jurassic bivalves. It is noteworthy that the deposit

994　feeding bivalve species, whose nutrition comes from within-sediment organic

995　detritus, do not show the increasing sizes seen amongst suspension feeding

996　bivalves. This trend could reflect an increased total abundance of suspended organic

997　matter at the seafloor or a change in the quality of the organic matter to larger

998　planktonic forms such as dinoflagellates. The works of van de Schootbrugge and

999　colleagues (van de Schootbrugge et al., 2007; van de Schootbrugge and Gollner,

1000　2013) suggest major changes amongst algal communities during the early

1001　Hettangian when green algae dominated. The latter provide poor-quality food for

1002　bivalves because of their small size and lack of essential nutrients (Brown et al.,

1003　1997; von Elert et al., 2003; Weiss et al., 2007). The intervals of green algal

1004 dominance also coincided with periods of black shale deposition (van de
1005 Schootbrugge et al., 2013, 2007; Xu et al., 2017) suggesting a possible influence of
1006 redox conditions but, as shown above, prevalence of dysoxia/anoxia correlates with
1007 neither size trends, nor recovery dynamics (Atkinson and Wignall, 2019). This
1008 suggests that improved food supply/quality may be a key control on size. This
1009 hypothesis requires testing with further studies of algal composition in the Lower
1010 Jurassic from understudied, younger intervals.

1011

1012 5.3 Body size and biotic recovery

1013   The importance of the Lilliput Effect in producing small bodied assemblages in
1014 the aftermath of a mass extinction was recently questioned (Atkinson et al., 2019),
1015 owing to its requirement for a species to survive the extinction to be considered a
1016 true Lilliput (Urbanek, 1993). Instead the Brobdingnag Effect was proposed, whereby
1017 new species originate during recovery at small a size and subsequently increase in
1018 size, thereby producing not only the small faunas in the immediate aftermath but also
1019 the increasing size suggested as a feature of biotic recovery (Atkinson et al., 2019).
1020 Following the end-Triassic mass extinction the Brobdingnag Effect has been shown
1021 for 11 (possibly 12) bivalve species whilst the Lilliput Effect only occurred in two
1022 (possibly three). The Brobdingnag Effect therefore dominated in the aftermath of the
1023 end-Triassic mass extinction and, in conjunction with Cope's Rule, produced bivalve
1024 communities of increasingly large sizes.

1025   Size increase provides an indicator of marine recovery that is unconnected
1026 with other factors that have been used to monitor post-extinction progress. Thus,
1027 ecological tiering recovers rapidly, in the early Hettangian, whilst bivalve diversity

1028   increase continued into the Pliensbachian (Atkinson and Wignall, 2019; Hallam,

1029   1996). Body size increase follows neither of these trends and is clearly monitoring a

1030   different and under-explored aspect of environmental recovery or change. As

1031   discussed above, temperature may exert some control on body size although food

1032   supply is potentially more important. The role of such factors and their significance

1033   during the recovery from other extinction crises remains to be explored.

1034

1035   **6. Conclusions**

1036   The recovery of bivalve communities following the end-Triassic mass

1037   extinction saw substantial, intraspecific size increase amongst many bivalves that

1038   persisted for 17 Myr and saw some bivalves increase their size by up to 476%. Such

1039   trends have been traditionally attributed to the Lilliput Effect: – the stunting of species

1040   in the harsh environmental conditions of the extinction interval and their subsequent

1041   size increase during recovery. However, this effect was minor, only 2-3 Lilliput

1042   species were found, instead the size trend is caused by the Brobdingnag Effect: – a

1043   within-species size increase of newly originated taxa. The Brobdingnag effect has

1044   been demonstrated for 11 filter-feeding species displaying diverse lifestyles but is not

1045   manifest amongst the deposit-feeding bivalves. In conjunction with this, newly

1046   appearing species are also progressively larger, with some aspect of this relating to

1047   Cope's Rule evolution (seen also in ammonite lineages). The mollusc populations of

1048   the Hettangian show an increase in average and maximum body size that was

1049   followed by a phase of reduced body size, here referred to as the Sinemurian Small

1050   Episode, before renewed size increase during the Pliensbachian. The geographic

1051   distribution of theses size trends remains uncertain although the evidence available

1052 suggests that it occurred across much of the European shelf seas and possibly in the

1053 Tethys and Panthalassa oceans.

1054 Local environmental factors can be linked to size changes (small bivalves in the

1055 deeper, less well-ventilated waters, large bivalves in the ironstones) but they cannot

1056 explain secular trends in body size of both benthos and nekton. The size trends

1057 appear unrelated to temperature and redox trends but may link to improvements in

1058 food supply (both abundance and quality) available to filter-feeding bivalves. Body

1059 size trends in the aftermath of the end-Triassic mass extinction occurred over longer

1060 time scales compared to other recovery metrics such as diversity and ecological

1061 complexity, with the latter recovering in less than a million years (Atkinson and

1062 Wignall, 2019). Future investigations of long-term body size trends following other

1063 crises may reveal the legacy of such crises is considerably longer than appreciated.

1078

1079 References

1080   Aberhan, M., 1994. Early Jurassic bivalvia of northern Chile. Part 1. Subclasses

1081   Palaeotaxodonta, Pteriomorphia, and Isofilibranchia. Beringeria 13, 3–115.

1082   Alroy, J., 1998. Cope's Rule and the dynamics of body mass evolution in North

1083   American fossil mammals. Science. 280, 731–734.

1084   https://doi.org/10.1126/science.280.5364.731

1085   Atkinson, D., 1994. Temperature and organism size – a biological law for

1086   ectotherms? Adv. Ecol. Res. 25, 1–58. https://doi.org/10.1016/S0065-

1087   2504(08)60212-3

1088   Atkinson, D., Sibly, R.M., 1997. Why are organisms usually bigger in cold

1089   environments? Making sense of a life history puzzle. Trends Ecol. Evol. 12,

1090   235–239.

1091   Atkinson, J.W., Wignall, P.B., Morton, J.D., Aze, T., 2019. Body size changes in

1092   bivalves of the family Limidae in the aftermath of the end-Triassic mass

1093   extinction: the Brobdingnag Effect. Palaeontology 62, 561–582.

1094   https://doi.org/10.1111/pala.12415

1095   Atkinson, J.W., Wignall, P.B., 2019. How quick was marine recovery after the end-

1096   Triassic mass extinction and what role did anoxia play? Palaeogeogr.

1097   Palaeoclimatol. Palaeoecol. 528, 99–119.

1098   https://doi.org/10.1016/j.palaeo.2019.05.011

1099   Attrill, M.J., Hartnoll, R.G., Rice, A.L., Thurston, M.H., 1990. A depth-related

1100   distribution of the red crab, Geryon trispinosus (Herbst) [=G. tridens KrÃ‚yer]:

1101   indications of vertical migration. Prog. Oceanogr. 24, 197–206.

1102   Bailey, T.R., Rosenthal, Y., McArthur, J.M., van de Schootbrugge, B., 2003.

1103   Paleoceanographic changes of the Late Pliensbachian-Early Toarcian interval: a

1104   possible link to the genesis of an Oceanic Anoxic Event. Earth Planet. Sci. Lett.

1105   212, 307–320. https://doi.org/10.1016/S0012-821X(03)00278-4

1106   Barras, C.G., Twitchett, R.J., 2007. Response of the marine infauna to Triassic –

1107   Jurassic environmental change: Ichnological data from southern England.

1108   Palaeogeogr. Palaeoclimatol. Palaeoecol. 244, 223–241.

1109   https://doi.org/10.1016/j.palaeo.2006.06.040

1110   Batten, R.L., Stokes, W.M.L., 1986. Early Triassic gastropods from the Sinbad

1111   Member of the Moenkopi Formation, San Rafael Swell, Utah. Am. Musuem

1112   Novit. 1–33.

1113   Beerling, D.J., Berner, R.A., 2002. Biogeochemical constraints on the Triassic-

1114   Jurassic boundary carbon cycle event. Global Biogeochem. Cycles 16, 1–13.

1115   Bergmann, C., 1847. Ueber die Verhältnisse der Wärmeökonomie der Thiere zu

1116   ihrer Grösse. Grottinger Stud. 3, 595–708.

1117   Berke, S.K., Jablonski, D., Krug, A.Z., Roy, K., Tomašových, A., 2013. Beyond

1118   Bergmann's Rule: size–latitude relationships in marine bivalvia world-wide.

1119   Glob. Ecol. Biogeogr. 22, 173–183. https://doi.org/10.1111/j.1466-

1120   8238.2012.00775.x

1121   Blackburn, T.M., Gaston, K.J., Loder, N., 1999. Geographic gradients in body size: a

1122   clarification of Bergmann's Rule. Divers. Distrib. 5, 165–174.

1123   https://doi.org/10.1046/j.1472-4642.1999.00046.x

1124   Brayard, A., Nützel, A., Stephen, D.A., Bylund, K.G., Jenks, J., Bucher, H., 2010.

1125   Gastropod evidence against the Early Triassic Lilliput Effect. Geology 38, 147–

1126   150. https://doi.org/10.1130/g30553.1

1127   Brom, K.R., Salamon, M.A., Ferré, B., Brachaniec, T., Szopa, K., 2015. The Lilliput

1128   Effect in crinoids at the end of the Oceanic Anoxic Event 2: a case study from

1129   Poland. J. Paleontol. 89, 1076–1081.

1130   Brown, M.R., Jeffrey, S.W., Volkman, J.K., Dunstan, G.A., 1997. Nutritional

1131   properties of microalgae for mariculture. Aquaculture 151, 315–331.

1132   Carey, N., Sigwart, J.D., 2014. Size matters: plasticity in metabolic scaling shows

1133   body-size may modulate responses to climate change. Biol. Lett. 10.

1134   https://doi.org/DOI: 10.1098/rsbl.2014.0408

1135   Caswell, B.A., Dawn, S.J., 2019. Recovery of benthic communities following the

1136   Toarcian oceanic anoxic event in the Cleveland Basin, UK. Palaeogeogr.

1137   Palaeoclimatol. Palaeoecol. 521, 114–126.

1138   https://doi.org/10.1016/j.palaeo.2019.02.014

1139   Chen, J., Song, H., He, W., Tong, J., Wang, F., Wu, S., 2019. Size variation of

1140   brachiopods from the Late Permian through the Middle Triassic in South China:

1141   Evidence for the Lilliput Effect following the Permian-Triassic extinction.

1142   Palaeogeogr. Palaeoclimatol. Palaeoecol. 519, 248–257.

1143   https://doi.org/10.1016/j.palaeo.2018.07.013

1144   Clémence, M.-E., Hart, M.B., 2013. Proliferation of Oberhauserellidae during the

1145   recovery following the Late Triassic extinction: paleoecological implications. J.

1146   Paleontol. 87, 1004–1015. https://doi.org/10.1666/13-021

1147   Cope, E.D., 1887. The origin of the fittest . D. Appleton and Co., New York.

1148   Copestake, P., Johnson, B., 2014. Lower Jurassic Foraminifera from the Llanbedr

1149   (Mochras Farm) borehole, north Wales, UK. Monograph of the

1150   Palaeontographical Society, London.

1151   Damborenea, S.E., 1987a. Early Jurassic bivalvia of Argentina. Part 1:

1152   stratigraphical introduction and superfamilies Nuculanacea, Arcacea, Mytilacea

1153   and Pinnacea. Palaeontogr. Abteilung A 199, 23–111.

1154   Damborenea, S.E., 1987b. Early Jurassic bivalvia of Argentina. Part 2: superfamilies

1155   Pteriacaea, Buchiacea and part of Pectinacea. Palaeontogr. Abteilung A 199,

1156   113–216.

1157   Damborenea, S.E., 2002. Early Jurassic bivalvia of Argentina. Part 3: superfamilies

1158   Monotoidea, Pectinoidea, Plicatuloidea and Dimyoidea. Palaeontogr. Abteilung

1159   A 265, 1–119.

1160   Damborenea, S.E., Echevarría, J., Ros-Franch, S., 2017. Biotic recovery after the

1161   end-Triassic extinction event: Evidence from marine bivalves of the Neuquén

1162   Basin, Argentina. Palaeogeogr. Palaeoclimatol. Palaeoecol. 487, 93–104.

1163   https://doi.org/10.1016/j.palaeo.2017.08.025

1164   Deconinck, J., Hesselbo, S.P., Debuisser, N., Averbuch, O., 2003. Environmental

1165   controls on clay mineralogy of an Early Jurassic mudrock (Blue Lias Formation,

1166   southern England). Int. J. Earth Science (Geol Rundsch) 92, 255–266.

1167   https://doi.org/10.1007/s00531-003-0318-y

1168   Dera, G., Pellenard, P., Neige, P., Deconinck, J., Pucéat, E., Dommergues, J., 2009.

1169   Distribution of clay minerals in Early Jurassic Peritethyan seas: palaeoclimatic

1170   significance inferred from multiproxy comparisons. Palaeogeogr. Palaeoclimatol.

1171   Palaeoecol. 271, 39–51. https://doi.org/10.1016/j.palaeo.2008.09.010

1172   Dommergues, J.-L., Montuire, S., Neige, P., 2002. Size patterns through time: the

1173   case of the Early Jurassic ammonite radiation. Paleobiology 28, 423–434.

1174   https://doi.org/10.1666/0094-8373(2002)028<0423:SPTTTC>2.0.CO;2

1175   Donovan, D.T., Curtis, M.L.K., Fry, T.R., 2005. The lower part of the Lias Group in

1176   south Gloucestershire: zonal stratigraphy and structure. Proc. Geol. Assoc. 116,

1177   45–59. https://doi.org/10.1016/S0016-7878(05)80016-1

1178 Gallois, R.W., 2008. The lithostratigraphy of the Shales-with-Beef Member of the

1179   Charmouth Mudstone Formation, Lower Jurassic. Proc. Ussher Soc. 12, 32–40.

1180 Gallois, R.W., 2009. Lithostratigraphy of the Penarth Group (Late Triassic) of the

1181   Severn Esturary area. Geosciences in south-west England. 12, 71-84.

1182 Gómez, J.J., Comas-rengifo, M.J., Goy, A., 2016. Palaeoclimatic oscillations in the

1183   Pliensbachian (Early Jurassic) of the Asturian Basin (northern Spain). Clim. Past

1184   12, 1199–1214. https://doi.org/10.5194/cp-12-1199-2016

1185 Hallam, A., 1960. A sedimentary and faunal study of the Blue Lias of Dorset and

1186   Glamorgan. Philos. Trans. R. Soc. London B Biol. Sci. 243, 1–44.

1187   https://doi.org/10.1098/rstb.1960.0003

1188 Hallam, A., 1963. Observations on the palaeoecology and ammonite sequence of

1189   the Frodingham Ironstone (Lower Jurassic). Palaeontology 6, 554–574.

1190 Hallam, A., 1965. Environmental causes of stunting in living and fossil marine

1191   benthonic invertebrates. Palaeontology 8, 132–155.

1192 Hallam, A., 1968. Morphology, palaeoecology and evolution of the genus Gryphaea

1193   in the British Lias. Philos. Trans. R. Soc. London B Biol. Sci. 254, 91–128.

1194   https://doi.org/10.1098/rstb.1968.0014

1195 Hallam, A., 1975. Evolutionary size increase and longevity in Jurassic bivalves and

1196   ammonites. Nature 258, 493–496.

1197 Hallam, A., 1978. How rare is phyletic gradualism and what is its evolutionary

1198   significance? Evidence from Jurassic bivalves. Paleobiology 4, 16–25.

1199 Hallam, A., 1996. Recovery of the marine fauna in Europe after the end-Triassic and

1200   early Toarcian mass extinctions. Geol. Soc. London, Spec. Publ. 102, 231–236.

1201   https://doi.org/10.1144/GSL.SP.1996.001.01.16

1202 Hallam, A., 2002. How catastrophic was the end-Triassic mass extinction? Lethaia

1203   35, 147–157.

1204 Hallam, A., Bradshaw, M.J., 1979. Bituminous shales and oolitc ironstones as

1205   indicators of transgressions and regressions. J. Geol. Soc. London 136, 157–

1206   164. https://doi.org/10.1144/gsjgs.136.2.0157

1207 Hallam, A., El Shaarawy, Z., 1982. Salinity reduction of the end-Triassic sea from the

1208   Alpine region into northwestern Europe. Lethaia 15, 169–178.

1209   https://doi.org/10.1111/j.1502-3931.1982.tb01136.x

1210 Hammer, Ø., Harper, D.A.T., Ryan, P.D., 2001. Past: Paleontological Statistics

1211   software package for education and data analysis.

1212 Harries, P.J., Knorr, P.O., 2009. What does the "Lilliput Effect" mean? Palaeogeogr.

1213   Palaeoclimatol. Palaeoecol. 284, 4–10.

1214   https://doi.org/10.1016/j.palaeo.2009.08.021

1215 Hesselbo, S.P., 2008. Sequence stratigraphy and inferred relative sea-level change

1216   from the onshore British Jurassic. Proc. Geol. Assoc. 119, 19–34.

1217   https://doi.org/10.1016/S0016-7878(59)80069-9

1218 Hesselbo, S.P., Jenkyns, H.C., 1998. British Lower Jurassic sequence stratigraphy,

1219   in: Mesozoic and Cenozoic sequence stratigraphy of European basins. SEPM

1220   Special Publications No. 60.

1221 Hesselbo, S.P., Oates, M.J., Jenkyns, H.C., 1998. The Lower Lias Group of the

1222   Hebrides Basin. Scottish J. Geol. 34, 23–60.

1223   Hesselbo, S.P., Robinson, S.A., Surlyk, F., 2004. Sea-level change and facies

1224   development across potential Triassic-Jurassic boundary horizons , SW Britain.

1225   J. Geol. Soc. London. 161, 365–379.

1226   His, E., Robert, R., Dinet, A., 1989. Combined effects of temperature and salinity on

1227   fed and starved larvae of the Mediterranean mussel Mytilus galloprovincialis and

1228   the Japanese oyster Crassostrea gigas. Mar. Biol. 100, 455–463.

1229   Hodges, P., 2000. The Early Jurassic bivalvia from the Hettangian and lower

1230   Sinemurian of south-west Britain part 1. Monograph of the Palaeontographical

1231   Society, London.

1232   Howard, A.S., 1985. Lithostratigraphy of the Staithes Sandstone and Cleveland

1233   Ironstone formations (Lower Jurassic) of north-east Yorkshire. Proc. Yorksh.

1234   Geol. Soc. 45, 261–275. https://doi.org/10.1144/pygs.45.4.261

1235   Howarth, M.K., 1955. Domerian of the Yorkshire coast. Proc. Yorksh. Geol. Soc. 30,

1236   147–175.

1237   Ivimey-Cook, H.C., 1971. Stratigraphical palaeontology of the Lower Jurassic of the

1238   Llanbedr (Mochras Farm) Borehole, in: Woodland, A.W. (Ed.), The Llanbedr

1239   (Mochras Farm) Borehole. Institute of Geological Sciences Report No.71/18, pp.

1240   87–92.

1241   Ivimey-Cook, H.C., 1975. The stratigraphy of the Rhaetic and Lower Jurassic in

1242   eastern Antrim. Bull. Geol. Surv. Gt. Britain 50, 51–69.

1243   Jablonski, D., 1997. Body-size evolution in Cretaceous molluscs and the status of

1244   Cope's Rule. Nature 385, 250–252.

1245   James, F.C., 1970. Geographic size variation in birds and its relationship to climate.

1246   Ecology 51, 365–390. https://doi.org/10.2307/1935374

1247   Johnson, A., 1984. The palaeobiology of the bivalve families Pectinidae and

1248   Propeamussiidae in the Jurassic of Europe. Zitteliana, München.

1249   Johnson, A., 1994. Evolution of European Lower Jurassic Gryphaea (Gryphaea) and

1250   contemporaneous bivalves. Hist. Biol. 7, 167–186.

1251   Jones, D.S., Gould, S.J., 1999. Direct measurements of age in fossil Gryphaea: the

1252   solution to a classic problem in heterochrony. Paleobiology 25, 158–187.

1253   Kaariainen, J.I., Bett, B.J., 2006. Evidence for benthic body size miniaturization in

1254   the deep sea. J. Mar. Biol. Assoc. United Kingdom 86, 1339–1345.

1255   https://doi.org/10.1017/S0025315406014366

1256   Korte, C., Hesselbo, S.P., 2011. Shallow marine carbon and oxygen isotope and

1257   elemental records indicate icehouse-greenhouse cycles during the Early

1258   Jurassic. Paleoceanography 26, 1–18. https://doi.org/10.1029/2011PA002160

1259   Korte, C., Hesselbo, S.P., Jenkyns, H.C., Rickaby, R.E.M., Spotl, C., 2009.

1260   Palaeoenvironmental significance of carbon- and oxygen-isotope stratigraphy of

1261   marine Triassic-Jurassic boundary sections in SW Britain. J. Geol. Soc. London.

1262   166, 431–445. https://doi.org/10.1144/0016-76492007-177

1263   Kosnik, M.A., Jablonski, D., Lockwood, R., Novack-Gottshall, P.M., 2006.

1264   Quantifying molluscan body size in evolutionary and ecological analyses:

1265   Maximizing the return on data-collection efforts. Palaios 21, 588–597.

1266   Lindström, S., van de Schootbrugge, B., Hansen, K.H., Pedersen, G.K., Alsen, P.,

1267   Thibault, N., Dybkjær, K., Bjerrum, C.J., Nielsen, L.H., 2017. A new correlation

1268   of Triassic–Jurassic boundary successions in NW Europe, Nevada and Peru,

1269   and the Central Atlantic Magmatic Province: A time-line for the end-Triassic

1270   mass extinction. Palaeogeogr. Palaeoclimatol. Palaeoecol. 478, 80–102.

1271   https://doi.org/10.1016/j.palaeo.2016.12.025

1272 Linse, K., Barnes, D.K.A., Enderlein, P., 2006. Body size and growth of benthic

1273   invertebrates along an Antarctic latitudinal gradient. Deep Sea Res. Part II Top.

1274   Stud. Oceanogr. 53, 921–931. https://doi.org/10.1016/j.dsr2.2006.03.006

1275 Loosanoff, V.L., Tommers, F.D., 1948. Effect of suspended silt and other substances

1276   on rate of feeding of oysters. Science. 107, 69–70.

1277   https://doi.org/10.1126/science.107.2768.69

1278 Mander, L., Twitchett, R.J., Benton, M.J., 2008. Palaeoecology of the Late Triassic

1279   extinction event in the SW UK. J. Geol. Soc. London. 165, 319–332.

1280   https://doi.org/10.1144/0016-76492007-029

1281 Márquez-aliaga, A., Damborenea, S., Gómez, J.J., Goy, A., 2010. Bivalves from the

1282   Triassic-Jurassic transition in northern Spain (Asturias and Western Basque-

1283   Cantabrian Basin). Ameghiniana 47, 185–205.

1284   https://doi.org/10.5710/AMGH.v47i2.3

1285 Martill, D.M., Vidovic, S.U., Howells, C., Nudds, J.R., 2016. The oldest Jurassic

1286   dinosaur: a basal neotheropod from the Hettangian of Great Britain. PLoS One

1287   11, e0145713. https://doi.org/10.1371/journal.pone.0145713

1288 McElwain, J.C., Beerling, D.J., Woodward, F.I., 1999. Fossil plants and global

1289   warming at the Triassic-Jurassic boundary. Science. 285, 1386–1391.

1290 Metcalfe, B., Twitchett, R.J., Price-Lloyd, N., 2011. Changes in size and growth rate

1291   of "Lilliput" animals in the earliest Triassic. Palaeogeogr. Palaeoclimatol.

1292   Palaeoecol. 308, 171–180. https://doi.org/10.1016/j.palaeo.2010.09.011

1293 Moghadam, H. V, Paul, C.R.C., 2000. Trace fossils of the Jurassic, Blue Lias, Lyme

1294   Regis, southern England. Ichnos 7, 283–306.

1295   https://doi.org/10.1080/10420940009380167

1296   Morton, N., 1989. Jurassic sequence stratigraphy in the Hebrides Basin, NW

1297   Scotland. Mar. Pet. Geol. 6, 243–260.

1298   Morton, N., Oates, M.J., 2004. The Hebrides Basin, in: Simms, M.J., Chidlaw, N.,

1299   Morton, N., Page, K.N. (Eds.), British Lower Jurassic Stratigraphy, Geological

1300   Conservation Review, Series No. 30. Joint Nature Conservation Committee,

1301   Peterborough, pp. 313–374.

1302   Munroe, D.M., Powell, E.N., Mann, R., Klinck, J.M., Hofmann, E.E., 2013.

1303   Underestimation of primary productivity on continental shelves: evidence from

1304   maximum size of extant surfclam (Spisula solidissima) populations. Fish.

1305   Oceanogr. 22, 220–233. https://doi.org/10.1111/fog.12016

1306   Nicol, D., 1967. Some characteristics of cold-water marine pelecypods. J. Paleontol.

1307   41, 1330–1340.

1308   Nori, L., Lathuiliére, B., 2003. Form and environment of Gryphaea arcuata. Lethaia

1309   36, 83–96. https://doi.org/10.1080/00241160310003081.

1310   Oates, M.J., 1978. A revised stratigraphy for the western Scottish Lower Lias. Proc.

1311   Yorksh. Geol. Soc. 42, 143–156.

1312   Olabarria, C., Thurston, M.H., 2003. Latitudinal and bathymetric trends in body size

1313   of the deep-sea gastropod Troschelia berniciensis (King). Mar. Biol. 143, 723–

1314   730. https://doi.org/10.1007/s00227-003-1116-6

1315   Payne, J.L., 2005. Evolutionary dynamics of gastropod size across the end-Permian

1316   extinction and through the Triassic recovery interval. Paleobiology 31, 269–290.

1317   Peck, L.S., Harper, E.M., 2010. Variation in size of living articulated brachiopods with

1318   latitude and depth. Mar. Biol. 157, 2205–2213. https://doi.org/10.1007/s00227-

1319   010-1486-5

1320 Radley, J.D., 2003. Warwickshire's Jurassic geology: past, present and future.

1321   Mercian Geol. 15, 209–218.

1322 Radulović, B., 2013. Lower Jurassic bivalves of eastern Serbia. Beringeria 43, 3–61.

1323 Rensch, B., 1948. Histological changes correlated with evolutionary changes of body

1324   size. Evolution (N. Y). 2, 218–230.

1325 Rhoads, D.C., Morse, J.W., 1971. Evolutionary and ecologic significance of oxygen-

1326   deficient marine basins. Lethaia 4, 413–428.

1327 Richmond, C., Marcus, N.H., Sedlacek, C., Miller, G.A., Oppert, C., 2006. Hypoxia

1328   and seasonal temperature: Short-term effects and long-term implications for

1329   Acartia tonsa dana. J. Exp. Mar. Bio. Ecol. 328, 177–196.

1330   https://doi.org/10.1016/j.jembe.2005.07.004

1331 Ros-Franch, S., Márquez-aliaga, A., Damborenea, S.E., 2014. Comprehensive

1332   database on Induan (Lower Triassic) to Sinemurian (Lower Jurassic) marine

1333   bivalve genera and their paleobiogeographic record. Paleontol. Contrib. 8, 1–

1334   219. https://doi.org/10.17161/PC.1808.13433

1335 Rosales, I., Quesada, S., Robles, S., 2004. Paleotemperature variations of Early

1336   Jurassic seawater recorded in geochemical trends of belemnites from the

1337   Basque-Cantabrian Basin, northern Spain. Palaeogeogr. Palaeoclimatol.

1338   Palaeoecol. 203, 253–275. https://doi.org/10.1016/S0031-0182(03)00686-2

1339 Ruhl, M., Deenen, M.H.L., Abels, H.A., Bonis, N.R., Krijgsman, W., Kürschner, W.M.,

1340   2010. Astronomical constraints on the duration of the Early Jurassic Hettangian

1341   Stage and recovery rates following the end-Triassic mass extinction (St Audrie's

1342   Bay / East Quantoxhead, UK). Earth Planet. Sci. Lett. 295, 262–276.

1343   https://doi.org/10.1016/j.epsl.2010.04.008

1344 Ruhl, M., Hesselbo, S.P., Hinnov, L., Jenkyns, H.C., Xu, W., Riding, J.B., Storm, M.,

1345   Minisini, D., Ullmann, C. V, Leng, M.J., 2016. Astronomical constraints on the

1346   duration of the Early Jurassic Pliensbachian Stage and global climatic

1347   fluctuations. Earth Planet. Sci. Lett. 455, 149–165.

1348   https://doi.org/10.1016/j.epsl.2016.08.038

1349 Sheppard, T.H., 2006. Sequence architecture of ancient rocky shorelines and their

1350   response to sea-level change: an Early Jurassic example from south Wales, UK.

1351   J. Geol. Soc. London 163, 595–606. https://doi.org/10.1144/0016-764920-015

1352 Shi, G.R., Zhang, Y.-C., Shen, S.-Z., He, W.-H., 2016. Nearshore-offshore-basin

1353   species diversity and body size variation patterns in Late Permian

1354   (Changhsingian) brachiopods. Palaeogeogr. Palaeoclimatol. Palaeoecol. 448,

1355   96–107. https://doi.org/10.1016/j.palaeo.2015.07.046

1356 Shirayama, Y., 1983. Size structure of deep-sea meio- and macrobenthos in the

1357   western Pacific. Int. Rev. der gesamten Hydrobiol. und Hydrogr. 68, 799–810.

1358 Simms, M.J., 2004. The Mendips and South Wales Massif, in: Simms, M.J., Chidlaw,

1359   N., Morton, N., Page, K.N. (Eds.), British Lower Jurassic Stratigraphy,

1360   Geological Conservation Review Series No. 30. Joint Nature Conservation

1361   Committee, Peterborough, pp. 112–156.

1362 Simms, M.J., Chidlaw, N., Morton, N., Page, K.N., 2004. British Lower Jurassic

1363   Stratigraphy, Geological Conservation Review Series, No. 30. Joint Nature

1364   Conservation committee, Peterborough.

1365 Simms, M.J., Jeram, A., 2007. Waterloo Bay, Larne, Northern Ireland: a candidate

1366   Global Stratotype Section and Point for the base of the Hettangian Stage and

1367   Jurassic System. ISJS Newsl. 34, 50–68.

1368   Simms, M.J., Page, K.N., 2004. The East Midlands Shelf, in: Simms, M.J., Chidlaw,

1369   N., Morton, N., Page, K.N. (Eds.), British Lower Jurassic Stratigraphy,

1370   Geological Conservation Review Series No. 30. Joint Nature Conservation

1371   Committee, Peterborough, pp. 215–223.

1372   Smith, C.R., Leo, F.C. De Leo, Bernardino, A.F., Sweetman, A.K., Arbizu, P.M.,

1373   2008. Abyssal food limitation, ecosystem structure and climate change. Trends

1374   Ecol. Evol. 23, 518–528. https://doi.org/10.1016/j.tree.2008.05.002

1375   Sogot, C.E., Harper, E.M., Taylor, P.D., 2014. The Lilliput Effect in colonial

1376   organisms: Cheilostome bryozoans at the Cretaceous-Paleogene mass

1377   extinction. PLoS One 9, e87048.

1378   Song, H., Tong, J., Chen, Z.-Q., 2011. Evolutionary dynamics of the Permian –

1379   Triassic foraminifer size: evidence for Lilliput Effect in the end-Permian mass

1380   extinction and its aftermath. Palaeogeogr. Palaeoclimatol. Palaeoecol. 308, 98–

1381   110. https://doi.org/10.1016/j.palaeo.2010.10.036

1382   Suan, G., Mattioli, E., Pittet, B., Lécuyer, C., Suchéras-marx, B., Duarte, L.V.,

1383   Philippe, M., Reggiani, L., Martineau, F., 2010. Secular environmental

1384   precursors to Early Toarcian (Jurassic) extreme climate changes. Earth Planet.

1385   Sci. Lett. 290, 448–458. https://doi.org/10.1016/j.epsl.2009.12.047

1386   Swift, A., 1999. Stratigraphy (including biostratigraphy), in: Swift, A., Martill, D.M.

1387   (Eds.), Fossils of the Rhaetian Penarth Group. The Palaeontological

1388   Association, London, pp. 15–30.

1389   Twitchett, R.J., 2007. The Lilliput Effect in the aftermath of the end-Permian

1390   extinction event. Palaeogeogr. Palaeoclimatol. Palaeoecol. 252, 132–144.

1391   https://doi.org/10.1016/j.palaeo.2006.11.038

1392   Urbanek, A., 1993. Biotic crises in the history of Upper Silurian graptoloids: A

1393   Palaeobiological model. Hist. Biol. 7, 29–50.

1394   https://doi.org/10.1080/10292389309380442

1395   van de Schootbrugge, B., Bachan, A., Suan, G., Richoz, S., Payne, J.L., 2013.

1396   Microbes, mud and methane: cause and consquence of recurrent Early Jurassic

1397   anoxia following the end-Triassic mass extinction. Palaeontology 56, 685–709.

1398   https://doi.org/10.1111/pala.12034

1399   van de Schootbrugge, B., Gollner, S., 2013. Altered primary productivity during

1400   mass-extinction events. Paleontol. Soc. Pap. 19, 87–114.

1401   van de Schootbrugge, B., Tremolada, F., Rosenthal, Y., Bailey, T.R., Feist-

1402   Burkhardt, S., Brinkhuis, H., Pross, J., Kent, D. V, Falkowski, P.G., 2007. End-

1403   Triassic calcification crisis and blooms of organic-walled "disaster species".

1404   Palaeogeogr. Palaeoclimatol. Palaeoecol. 244, 126–141.

1405   https://doi.org/10.1016/j.palaeo.2006.06.026

1406   Vermeij, G.J., 2011. Shifting sources of productivity in the coastal marine tropics

1407   during the Cenozoic era. Proc. R. Soc. London B 278, 2362–2368.

1408   https://doi.org/10.1098/rspb.2010.2362

1409   von Elert, E., Martin-creuzburg, D., Le Coz, J.R., 2003. Absence of sterols constrains

1410   carbon transfer between cyanobacteria and a freshwater herbivore (Daphnia

1411   galeata). Proc. R. Soc. London B 270, 1209–1214.

1412   https://doi.org/10.1098/rspb.2003.2357

1413   Wacker, A., von Elert, E., 2003. Food quality controls reproduction of the zebra

1414   mussel (Dreissena polymorpha). Ecophysiology 135, 332–338.

1415   https://doi.org/10.1007/s00442-003-1208-5

1416 Wacker, A., von Elert, E., 2008. Body size and food thresholds for zero growth in

1417   Dressena polymorpha: a mechanism underlying intraspecific competition.

1418   Freshw. Biol. 53, 2356–2363.

1419 Weedon, G.P., 1986. Hemipelagic shelf sedimentation and climatic cycles: The basal

1420   Jurassic (Blue Lias) of S. Britain. Earth Planet. Sci. Lett. 76, 321–335.

1421   https://doi.org/10.1016/0012-821X(86)90083-X

1422 Weedon, G.P., 1987. Palaeoclimatic significance of open-marine cyclic sequences.

1423   Linacre College.

1424 Weedon, G.P., Jenkyns, H.C., Page, K.N., 2018. Combined sea-level and climate

1425   controls on limestone formation, hiatuses and ammonite preservation in the Blue

1426   Lias Formation, south Britain (uppermost Triassic–Lower Jurassic). Geol. Mag.

1427   155, 1117–1149. https://doi.org/10.1017/S001675681600128X

1428 Weedon, G.P., Page, K.N., Jenkyns, H.C., 2019. Cyclostratigraphy, stratigraphic

1429   gaps and the duration of the Hettangian Stage (Jurassic): insights from the Blue

1430   Lias Formation of southern Britain. Geol. Mag. 156, 1469–1509.

1431   https://doi.org/10.1017/S0016756818000808

1432 Weiss, M.B., Curran, P.B., Peterson, B.J., Gobler, C.J., 2007. The influence of

1433   plankton composition and water quality on hard clam (Mercenaria mercenaria)

1434   populations across Long Island's south shore lagoon estuaries (New York,

1435   USA). J. Exp. Mar. Bio. Ecol. 345, 12–25.

1436 Wiest, L.A., Lukens, W.E., Peppe, D.J., Driese, S.G., Tubbs, J., 2018. Terrestrial

1437   evidence for the Lilliput Effect across the Cretaceous-Paleogene (K-Pg)

1438   boundary. Palaeogeogr. Palaeoclimatol. Palaeoecol. 491, 161–169.

1439   https://doi.org/10.1016/j.palaeo.2017.12.005

1440 Wignall, P.B., 1990. Benthic palaeocology of the Late Jurassic Kimmeridge Clay of

1441   England. Spec. Pap. Palaeontol. 43, 64.

1442 Wignall, P.B., 2001. Sedimentology of the Triassic-Jurassic boundary beds in Pinhay

1443   Bay (Devon, SW England). Proc. Geol. Assoc. 112, 349–360.

1444   https://doi.org/10.1016/S0016-7878(01)80014-6

1445 Wignall, P.B., Bond, D.P.G., 2008. The end-Triassic and Early Jurassic mass

1446   extinction records in the British Isles. Proc. Geol. Assoc. 119, 73–84.

1447   https://doi.org/10.1016/S0016-7878(08)80259-3

1448 Wignall, P.B., Hallam, A., 1991. Biofacies, stratigraphic distribution and depositional

1449   models of British onshore Jurassic black shales. Geoogical Soc. Spec. Publ. 58,

1450   291–309.

1451 Wotzlaw, J., Guex, J., Bartolini, A., Gallet, Y., Krystyn, L., McRoberts, C.A., Taylor,

1452   D., Schoene, B., Schaltegger, U., 2014. Towards accurate numerical calibration

1453   of the Late Triassic: High-precision U-Pb geochronology constraints on the

1454   duration of the Rhaetian. Geology. https://doi.org/10.1130/G35612.1

1455 Xu, W., Ruhl, M., Hesselbo, S.P., Riding, J.B., Jenkyns, H.C., 2017. Orbital pacing of

1456   the Early Jurassic carbon cycle, black-shale formation and seabed methane

1457   seepage. Sedimentology 64, 127–149. https://doi.org/10.1111/sed.12329